Gyrator-Capacitor Modeling Approach to Study the Impact of Geomagnetically Induced Current on Single-Phase Core Transformer

A Thesis Presented for the

Master of Science

Degree

The University of Tennessee, Knoxville

Parul Kaushal

May 2017

Copyright © 2017 by Parul Kaushal

All rights reserved.

DEVOTION

This thesis is devoted to my husband, Vishal Sharma, and to my entire family for their sustained support throughout my educational endeavors.

ACKNOWLEDGEMENTS

It gives me immense pleasure to express my sincere and whole hearted gratitude to Dr. Syed Kamrul Islam for his endless guidance, invaluable and untiring help, encouraging attitude and supervision throughout my research work at the University of Tennessee.

I am thankful to Dr. Marcus Aaron Young of Mitsubishi for endless discussions to achieve my final goal and for his indefatigable support.

My heartfelt thanks go to Dr. Yilu Liu and Dr. Benjamin J Blalock in serving as a member of my thesis committee.

I would also like to acknowledge Oak Ridge National Laboratory (ORNL) for providing financial support for my graduate education.

ABSTRACT

Among various approaches used for determining the behavior of power transformers to model the geomagnetically induced current (GIC), the gyrator-capacitor approach is proposed. This approach offers a better understanding of magnetic components compared to other methods, particularly for multi-winding devices and is used to model GIC in a single-phase core type power transformer. In the gyrator-capacitor approach, the gyrator acts as a bridge between the electric and the magnetic circuits making it possible to simulate the two circuits simultaneously.

Under GIC conditions, the transformer core suffers a half-cycle saturation, which is the main cause of the disturbances in the power system. In addition, the design of the transformer core is one of the other important factor to analyze the impact of GIC, as the single-phase and the three-phase transformers have different core design. The single-phase transformers are known to be more susceptible to GIC than their three-phase counterparts and even a small range of DC is sufficient to drive the core of a single-phase transformer in the saturation region. The behavior of single-phase transformer is analyzed as half-cycle saturation in the fluxes, following the simulations achieved for voltages, magnetizing current, exciting current and harmonics at different levels of DC by using different magnitude of GIC (increasing order). The harmonics obtained from the proposed approach are validated with the previously published research for single-phase transformers experiencing half-cycle saturation. Since the GIC affects the current waveforms and therefore, the deviation of the current waveform is also calculated in the form of total harmonic distortion (THD).To model a transformer using the gyrator-capacitor approach, P-SPICE software tool is used.The results from the analysis reveal that, the behavior of the transformer model is dependent on the source impedance and the half-cycle saturation is dependent on the DC source setting.

TABLE OF CONTENTS

CHAPTER 1
INTRODUCTION AND GENERAL INFORMATION 1
1.1 Overview 1
1.2 Thesis Outline 5
CHAPTER 2
SINGLE-PHASE TRANSFORMER CONCEPT AND LITERATURE REVIEW 6
2.1 Single-Phase Transformer Concept 6
2.2 Literature Review 8
CHAPTER 3
MODELING APPROACHES AND THE PROPOSED APPROACH 10
3.1 Modeling Approaches 10
CHAPTER 4
SINGLE-PHASE TRANSFORMER MODELING USING GYRATOR-CAPACITOR APPROACH 22
4.1 Single-Phase Transformer Gyrator-Capacitor Model 22
CHAPTER 5
SIMULATION RESULTS 29
5.1 Transformer Behavior Without GIC (DC) 29
5.1.1 Input /Output Voltage Waveform in the Presence of Small Source Impedance 30
5.1.2 Input /Output Current Waveform in the Presence of Small Source Impedance 30
5.1.3 Input /Output Voltage Waveform in the Presence of Large Source Impedance 31
5.1.4 Input /Output Current Waveform in the Presence of Large Source Impedance 32
5.1.5 Flux Waveform 33
5.1.6 Magnetizing Current Waveform 34
5.2 Transformer Behavior With GIC(DC) 35
5.2.1 Flux Waveform 35
5.2.2 Exciting Current Waveform 38
5.2.3 Exciting Current Harmonics 41
5.2.4 Output Waveform 43

CHAPTER 6
CONCLUSIONS AND FUTURE WORK **46**

REFERENCES **47**
APPENDIX **51**
VITA **55**

LIST OF TABLES

Table 3.1: Force and Flow Variables in Electric/Magnetic Domain. 12
Table 3.2: Comparison of the Force and the Flow Variables in Electric /Magnetic Domain..... 14
Table 3.3: Analogs of Electric and Magnetic Quantities. 21

LIST OF FIGURES

Figure 1.1.1:Transformer core operating under GIC conditions. 4
Figure 1.1.2: Magnetizing current during half-cycle saturation. 4
Figure 2.1.1:Schematic of a basic single-phase transformer. 7
Figure 3.1.1: Reluctance-resistance approach for magnetic circuit modeling. 12
Figure 3.1.2: Permeance-capacitance approach for magnetic circuit modeling. 14
Figure 3.1.3: Schematic representation of a gyrator. 16
Figure 3.1.4: Gyrator link. 16
Figure 3.1.5: Gyrator-capacitor model for magnetic circuit modelling. 18
Figure 3.1.6 : Gyrator-capacitor model with variable permeance. 18
Figure 3.1.7 :Nonlinear permeance (Variable Permeance) application in P-SPICE. 20
Figure 4.1 : A gyrator-capacitor model with variable permeance for the single-phase winding transformer. 23
Figure 4.2.1 :Variable permeance block implemnted in P-SPICE. 23
Figure 4.2.2 : Flux calculation circuit in P-SPICE. 24
Figure 4.2.3 :Gyrator-capacitor model for two winding core transformer in P-SPICE. 26
Figure 4.2.4 : AC electric circuits (Primary and Secondary Side) in P-SPICE. 27
Figure 4.2.5 : DC electric circuit in P-SPICE. 28
Figure 4.2.6 : AC secondary side electric circuit (Open Circuit) in P-SPICE. 28
Figure 5.1.1: I/O voltage waveform in the presence of small source impedance. 30
Figure 5.1.2: I/O current waveform in the presence of small source impedance……..31
Figure 5.1.3: I/O voltage waveform in the presence of large source impedance..... 32
Figure 5.1.4: I/O Current waveform in the presence of large source impedance. 32
Figure 5.1.5: Flux waveform in the presence of large source impedance without GIC(DC). 34
Figure 5.1.6: Magnetizing waveform in the presence of large source impedance without GIC(DC). 34
Figure 5.2.1.1: Flux waveform for 10A GIC(DC) in the presence of large source impedance.... 36
Figure 5.2.1.2: Flux waveform for 100A GIC(DC) in the presence of large source impedance.. 36
Figure 5.2.1.3: Flux waveform for 300A GIC(DC) in the presence of large source impedance.. 37
Figure 5.2.1.4: Flux waveform for 500A GIC(DC) in the presence of large source impedance.. 37
Figure 5.2.1.5: Flux waveform for 700A GIC(DC) in the presence of large source impedance.. 38
Figure 5.2.2.1: Exciting current waveform for 11.5A GIC(DC)[13]..... 39
Figure 5.2.2.2: Exciting current waveform for 10A GIC(DC). 39
Figure 5.2.2.3: Exciting current waveform for 50A GIC(DC). 40
Figure 5.2.2.4: Exciting current waveform for 100A GIC(DC). 40
Figure 5.2.3.1: Exciting current harmonics for 10A GIC(DC). 41
Figure 5.2.3.2: Exciting current harmonics for 50A GIC(DC). 42
Figure 5.2.3.3: Exciting current harmonics for 100A GIC(DC). 42
Figure 5.2.3.4: Exciting current harmonics for 11.5A GIC(DC) [13]. 43
Figure 5.2.4.1: Output waveform for 50A GIC(DC). 44
Figure 5.2.4.2: Output waveform for 100A GIC(DC). 44

Figure 5.2.4.3: Output waveform for 250A GIC(DC). 44
Figure 5.2.4.4: Output waveform for 500A GIC(DC). 45

CHAPTER 1

INTRODUCTION AND GENERAL INFORMATION

1.1 Overview

The electric power system provides a reliable, secure and stable delivery of electric power, which relies on working of the major electric components such as generators, transmission lines and transformers. Electricity is generated at power plants or generating stations using primary sources of energy such as oil, coal, natural gas, hydropower, solar, wind, or other methods. Step-up transformers located at the generating plants steps up the voltage levels to make electric power suitable for economical, low-loss, long-distance transmission to regional locations. Primary customers (e.g., heavy industry) may take power at transmission-level voltages, but most commercial and all residential services require voltages at distribution levels. Therefore, the step-down transformers located at points along the transmission network step-down the high voltage electricity to distribution levels that are fit for residential, commercial and industrial use. Finally, the transformers are mounted on the poles or within the buildings to lower the distribution voltage levels even further for secondary customers that include individual homes and businesses. Substations play a pivotal role in bulk electric systems and typically support large power transformers that provide the step-up and the step-down of voltages throughout the network. However, substations have additional functions that include line switching, conversion from AC to high voltage direct current (HVDC), and reactive support.

Today's electric power system is vulnerable to number of threats such as natural threats due to weather, as well as other threats such as terrorism or cyber threat. Solar storm or geomagnetic

disturbance (GMD) is one of the threats that occurs due to the change in space conditions and if GMD is sufficient enough, it can result into the disruption of normal operation of the power system and can end in loss of power for hours or days.

In March 1989, a geomagnetic disturbance (GMD) occurred in Hydro-Quebec system and left a huge impact on North America grid, leaving six million people out of power for nine hours [1]. The main source of GMD is the Sun, as it continuously emits large mass of charged solar energetic particles and solar wind ions. These charged particles interact with the earth's magnetosphere and produce very high ampere current, also known as electro jets. These electro jets induce a geo-electric field in earth, symbolized as an ideal voltage source, connected in series with the transmission lines which acts as an electromotive force (emf), resulting in Geomagnetically Induced Currents (GIC). The geo-electric field has a lower frequency range of 0.001-0.1Hz and therefore GIC is treated as quasi-DC currents. Conducting paths in bulk electric power systems such as transmission lines and pipe lines allow GICs to enter the power system which may cause DC bias in the ferromagnetic devices. DC bias may affect the transformer, resulting in a DC offset flux in the core. This in turn causes the half-cycle saturation of flux in the core, which injects a significant amount of even and odd harmonic currents, also known as harmonics, into the power system. As a result of these harmonics, the protection and the controlling equipments of power system may trip, leading to disturbances in the system voltage regulation and stability. Figure 1.1.1 shows the characteristics of the transformer core and the relationship among the core flux and the magnetizing current under GIC conditions. Figure 1.1.1(a) shows, the core flux as a function of time with and without the DC flux, the flux with respect to current corresponding to AC and (AC+DC) flux and the magnetizing current with and without DC flux. The DC flux shows the half-cycle saturation in the magnetizing current (I_mDC).

When GIC (quasi-DC) flows in the transformer, it produces a DC flux and adds on the normal AC flux during the half cycle (50 or 60Hz) and subtracts from the AC flux during the other half cycle, resulting in the shifting of operating point of the magnetizing characteristics resulting in a DC flux offset. Until the core flux remains below the knee point, the transformer core operates in the linear part of the saturation curve and as it starts moving beyond the knee point, the core flux enters into the saturation region and the magnetizing current increases. With a DC flux off set, the magnetizing current (I_mDC) is neither symmetrical nor sinusoidal and may have positive or negative peaks on either side of the cycle but not on both sides of the cycle as shown in Figure 1.1.2 and the phenomenon is known as half-cycle saturation.

Motivation

To maintain stability in the system, it is important to overcome the GMD events. Transformers being main component in a power system, absorb high level of GIC which results in heating of windings and harmonic distortions. Due to these distortions in waveforms, control and protecting equipments may trip the system. Therefore, in order to maintain uninterrupted functioning of power system, it is important to understand the impact of GIC using simulation tools. For this study, P-SPICE is used for transformer GIC modeling by using simple gyrator-capacitor approach.

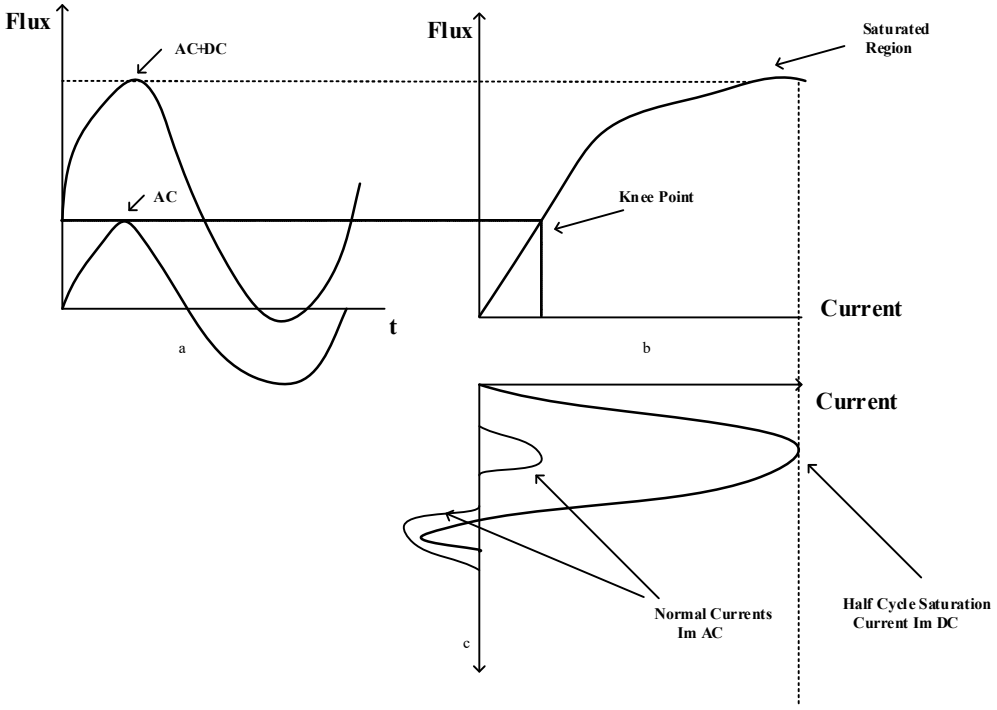


Figure 1.1.1:Transformer core operating under GIC conditions.

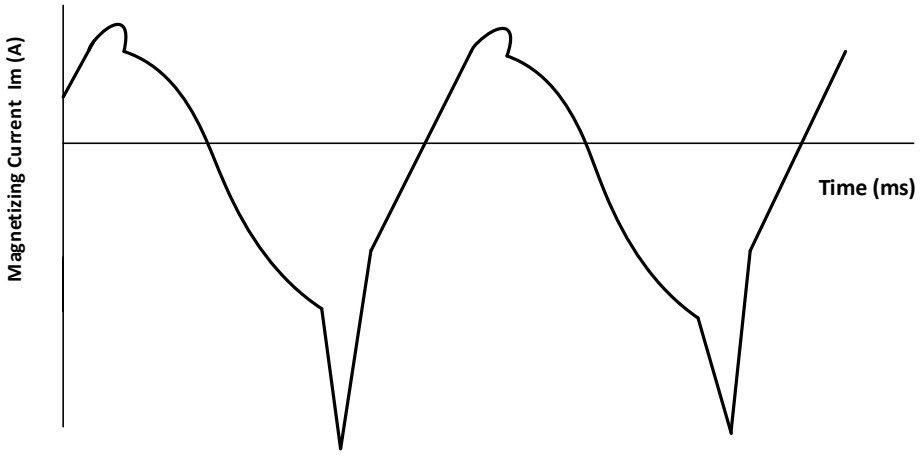


Figure 1.1.2: Magnetizing current during half-cycle saturation.

1.2 Thesis Outline

The structure of this thesis is as follows: Chapter 2 presents the concept for single-phase transformer and literature review of the models used to study the GIC impacts on transformers. Chapter 3 discusses different approaches to model the magnetic components from the electric components and the proposed gyrator-capacitor approach is also presented. Chapter 4 presents the application of the gyrator-capacitor method to model GIC for a single-phase transformer. Chapter 5 shows the results obtained from the simulation using single-phase transformer gyrator-capacitor model. Finally, conclusion and future work are summarized in Chapter 6.

CHAPTER 2

SINGLE-PHASE TRANSFORMER CONCEPT AND LITERATURE REVIEW

2.1 Single-Phase Transformer Concept

A single-phase transformer consists of two coils of wire also known as the primary winding and the secondary winding. The windings in the transformer are not electrically connected but are linked magnetically and operate on the principles of induction. In this process, a coil or a winding magnetically induces a voltage on the another winding located in close proximity to it. The core is made up of laminations connected together to reduce the coreloss (eddy current loss). When a sinusoidal voltage is applied in the primary winding, a current start to flow in the coil which sets up a magnetic field. As the current starts to build up, the magnetic field starts rising and the magnetic field lines starts expanding outward from the coil, for which the core forms the path and results in magnetic flux. These magnetic lines of flux tend to flow in the secondary winding and induce a voltage on the secondary winding.

The expression below shows that the voltage in transformer, depends on the number of turns in the coil and the current in the windings as,

$$\frac{Vs}{Vp} = \frac{Ns}{Np} = \frac{Ip}{Is} \quad \text{.....(2.1)}$$

Where, V_p is the voltage in the primary winding,V_s is the voltage in the secondary winding, N_p is the number of turns in the primary winding, N_s is the number of turns in the secondary winding,I_p is the current flowing in the primary winding, and I_s is the current flowing in the secondary winding.

A single-phase transformer can be used to either increase or decrease the secondary voltage with respect to the primary voltage. If a transformer secondary voltage increases with respect to the primary voltage , the transformer is known as Step-up transformer and if a voltage on the secondary side decreases with respect to primary voltage, the transformer is known as Step-down transformer .Typically, single-phase core transformer are Step-down type. A basic construction of single-phase transformer is shown in the Figure 2.1.1.

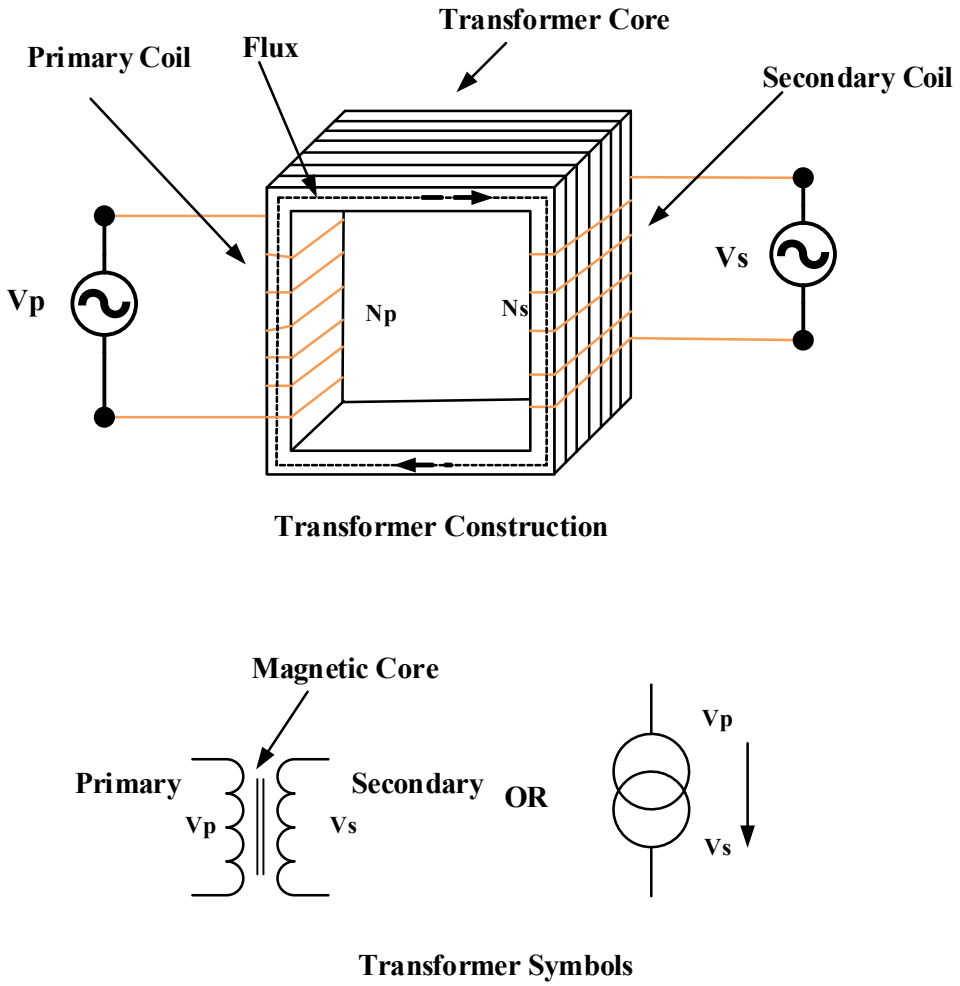


Figure 2.1.1:Schematic of a basic single-phase transformer.

2.2 Literature Review

The impact of geomagnetically induced current on the transformers has been reported and it has been widely accepted that a single-phase transformer is more vulnerable to GICs than its three-phase counterpart. An analytical approach and a time domain simulation to investigate the operating condition of a single-phase transformer under steady state and quasi-DC transient of the geo-magnetically induced current (GIC) have been reported [2]. The analytical approach used in the paper employs a two-slope piece-wise linear magnetization characteristics and facilitates the development of generic characteristics of the system to study the methods to reduce the risk of the power system instability and blackout during a geomagnetic disturbance (GMD). The results show that the reactive power of the transformer increases with GIC with an initial slope of 2.0, which is equal to the transformer AC peak voltage on a per unit basis. The results obtained are compared with the Hydro One SVC single phase transformers of rating 500kV and 230kV respectively [3]. Investment Planning Division of Hydro One Networks Inc., Ottawa in collaboration with ANF Energy Solutions Inc., Ottawa has also developed a real time simulator for providing real time simulations of GIC. This real time simulator uses magnetic field data from Ottawa Magnetic Observatory which is used with an earth model to calculate the electric field at the earth's surface and the results are displayed in the form of set of tables and graphs [4]. Similar type of research work has been done in Finland by Finnish Meteorological Institute (FMI) to develop theoretical models for estimating the risks to the electric grid due to GIC [5]. Some researchers used mathematical models incorporating electric and magnetic circuits to predict the current flux waveforms [6]. The GIC also affects the winding of transformers in the form of heating [7], when a large segment of flux leaks out beyond the core and the winding assembly. IEEE standard C57.91-1995 [8] provides some guidance on the

temperature limit that should not be exceeded in either winding. GIC disturbs the current waveform and produces even and odd harmonics resulting in problems in the relay and the protective devices in the power system. The deviation of the waveforms is studied by using total harmonic distortion (THD) block in MATLAB [9]. The comparison of various core models under DC excitation using experimental analysis by geomagnetically induced currents has also been reported [10]. The DC excitation of transformer is studied experimentally using three-core models, and the results show that single-phase three-legged core is more susceptible to excitation effects than the three-phase three-legged core transformers. Several past studies have been dedicated to the impact of GIC on the transformers using various types of models [11,12]. These models often require complex finite element modeling (FEM) that requires detailed design information about the core, the mechanical structure, windings and the mechanical enclosures. The finite element analysis is computationally intensive and may require long simulation times. Some studies used different simulation methods to calculate the harmonics for exciting current and MVAR intake of the transformers resulting from GIC. To estimate the harmonics for exciting current for single- phase transformer, one research paper has presented a simplified method based on the equivalent magnetizing curve of the transformer [13]. Unlike the previous researches, this thesis represents a different approach (gyrator-capacitor approach) to observe its ability to model the impact of GIC on a single-phase transformer. In addition, this research effort attempts to validate the acquired simulation results such as exciting current waveforms and harmonics, with some of the past research work as no previous work has done using this approach on single-phase transformers.

CHAPTER 3

MODELING APPROACHES AND THE PROPOSED APPROACH

3.1Modeling Approaches

To model the magnetic components from electric components, three following approaches can be used:

1. Reluctance-resistance analogy
2. Permeance-capacitance analogy
3. Gyrator-capacitor analogy

Reluctance-resistance analogy is a conventional approach for modeling the magnetic circuit where lumped equivalent circuits are formed using resistors that represent flux path and voltage sources that represent magneto-motive force. The equivalent circuit for reluctance-resistance model is shown in Figure 3.1.1. In this figure, the analogy between the magnetic and the electric domains is illustrated, where resistors are used to represent the reluctance of the magnetic path ways described below:

$$R=l/\sigma A \quad \text{.....(3.1)}$$

$$\mathcal{R}=l/\mu A \quad \text{.....(3.2)}$$

Where, R is the electric resistance (Ω), $\mathcal{R}$ is the magnetic reluctance ($Henry^{-1}$), l is the mean length (m), A is the cross sectional area (m^2), σ is the electrical conductivity (Siemens/meter), and μ is the permeability (Henry/m).

In the electric circuit, the voltage represents the force variable that interacts with the resistance to develop the current, the flow variable, in accordance with the Ohm's Law is given by Equation (3.3). Similarly, the magneto-motive force or mmf, is the force variable that

interacts with the reluctance to develop the magnetic flux, the flow variable in the magnetic circuit and is described in Equation (3.4).

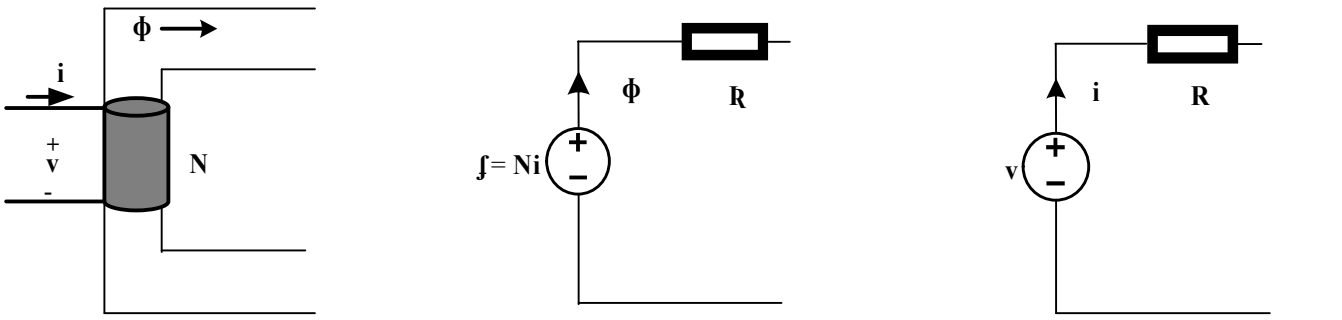
$$I=V/R \quad \text{.....(3.3)}$$

$$\phi=\int/R \quad \text{.....(3.4)}$$

Where, I is the current (Ampere), V is the voltage (V), ϕ is the flux (Wb) and $\int$ is the magneto motive force (Ampere-Turns).

Figure 3.1.1(a) shows a simple electromagnetic device consisting of winding and a core material of known type and geometry with current flowing through the winding. The winding has N number of turns. The equivalent magnetic circuit is shown in the Figure 3.1.1 (b), where the magneto-motive force is equal to Ni and the reluctance is determined by Equation (3.2). The reluctance and the resistance models are applied and the equivalent electric circuit as shown in Figure 3.1.1 (c). Table 3.1 shows the force and the flow variables in electric/magnetic circuit employing the reluctance-resistance approaches. It is evident from the table that, the products of the force and the flow variables are different in the electric and the magnetic domains.

For instance, the flow variable for the electric domain is the current which has the units of coulomb per second, whereas in the magnetic domain the flow variable is the flux which has the units of volt-second. Therefore, the reluctance-resistance approach for circuit modeling does not permit the energy transfer directly between the two domains due to the in-consistent flow variables. In addition, the authors have stated that it is hard to represent the inductive nature of the magnetic circuit that stores energy with component like resistors that dissipate energy [14].



(a) Electromagnetic Device (b) Equivalent Magnetic Circuit (c) Electric Circuit Analog

Figure 3.1.1: Reluctance-resistance approach for magnetic circuit modeling.

Table 3.1: Force and Flow Variables in Electric/Magnetic Domain.

Domain	Force Variable	Flow Variable	Force×Flow
Electric	Voltage(V)	Current(A)={C/s}	Power (V.A) ={W}
Magnetic	Mmf (A. turns)	Flux(Wb)= {V.s}	Energy (V.A.s) ={J}

The issues can be resolved by replacing the resistors (reluctance) with the capacitors (permeance) in the magnetic circuit. Using capacitors instead of resistors make the flow variable consistent for linking the domains and is known as **permeance-capacitance analogy.** In this analogy, flux can be expressed in terms of reluctance and mmf substituting the definition of reluctance from Equation (3.2) in Equation (3.4) we get,

$$\phi = \int / \mathcal{R} = (\mu A / l) \times \int \quad \text{(3.5)}$$

As previously explained, electric current is the flow variable in the electric domain and represents a time rate of change. As the magnetic flux is not represented by a time rate of change, it is possible to accomplish a flow variable consistent with the electric domain by taking the time derivative of Equation (3.5).The resulting flow variable is a time rate of change of flux and is expressed in Equation (3.6) below.

$$d\phi/dt = (\mu A/l) \times d\int/dt \quad \text{(3.6)}$$

The constant term in the above equation is known as permeance, which is equal to the inverse of reluctance as described in Equation (3.7) and is represented by.

$$P = (\mu A/l) = 1/\mathcal{R} \quad \text{(3.7)}$$

Where, $d\phi/dt$ is the time rate of change of flux (V·s/s) or (V) and $d\int/dt$ is the time rate of change of mmf (A·turns/s).

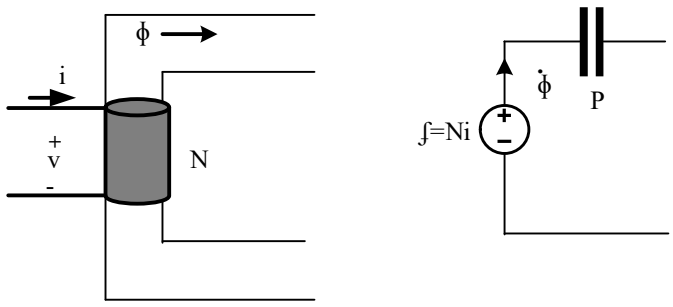
Both equations together represent the current through a capacitor and is expressed as follows.

$$\acute{\phi} = P \times d\int/dt \quad \text{(3.8)}$$

$$i = C \times dv/dt \quad \text{(3.9)}$$

Where,$\acute{\phi}$ is the time rate of change of flux (V·s/s) or (V), i is the current (A) and C is the capacitance (Farad).

Equations (3.8) and (3.9) both signify that the force variable for both the domains remain consistent and do not change from the reluctance-resistance approach. Therefore, the permeance -capacitance analogy utilizes the magnetomotive force, ∫, as an analog to electric voltage and is shown in the Figure 3.1.2.



(a) Electromagnetic Device (b) Permeance – Capacitance Circuit

Figure 3.1.2: Permeance-capacitance approach for magnetic circuit modeling.

The comparison of these approaches is given in the Table 3.2.

Table 3.2: Comparison of the Force and the Flow Variables in Electric /Magnetic Domain.

Domain	Force Variable	Flow Variable	Force×Flow
Electric	Voltage(V)	Current(A)={C/s}	Power (V.A) ={W}
Magnetic (Reluctance-Resistance)	Mmf (A. turns)	Flux(Wb)= {V.s}	Energy (V.A.s) ={J}
Magnetic (Permeance-Capacitance)	Mmf (A. turns)	Flux rate (Wb/s)= {V}	Power (V.A.turns) ={W}

The comparison reveals that the permeance-capacitance approach provides a force-flow product that is more consistent with the electric domain, but proportionally unequal to the electric circuit by the number of winding turns. This issue is resolved by considering the number of turns upon transfer of energy between the domains. With the matching force-flow products, it is possible to transfer energy between the domains. However, the transfer of energy will require an interface that performs the transfer and accounts for the proportionality issue.

Proposed Gyrator Capacitor Approach

In the gyrator-capacitor approach, the gyrator and the permeance-capacitance make energy transfer possible between the electric and the magnetic domains. Bernard Tellegen of the Philips Physics Laboratory first introduced the gyrator concept in 1948 [15]. The gyrator is an ideal, passive, two-port electrical circuit element that supports exchange of force and flow between two systems [16] as shown in the Figure 3.1.3.

The gyrator operates similar to an ideal transformer. However, a transformer relates the primary voltage to that of the secondary while the gyrator relates the primary voltage to the secondary current. Thus, an ideal transformer is formed by connecting two gyrators back-to-back. A constant of proportionality equalizes the energy on both sides. The relationship between the inputs and the outputs of the gyrator are expressed in Equation (3.10). Similar to an ideal transformer, a gyrator has no losses, in accordance with Equation (3.11), and thus no energy dissipates in the transformation process.

$$\begin{bmatrix} v1 \\ v2 \end{bmatrix} = \begin{bmatrix} 0 & -r \\ r & 0 \end{bmatrix} \times \begin{bmatrix} i1 \\ i2 \end{bmatrix} \quad \text{.....(3.10)}$$

$$v_1 i_1 + v_2 i_2 = 0 \quad \text{.....(3.11)}$$

Where, v_1 is the input voltage, v_2 is the output voltage, i_1 is the input current, i_2 is the output current and r is the constant of proportionality.

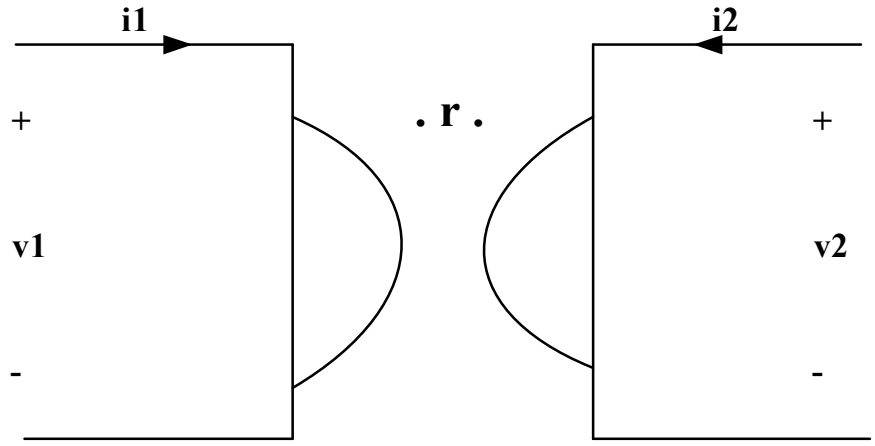


Figure 3.1.3: Schematic representation of a gyrator.

Figure 3.1.4 shows the application of gyrator to link the electric circuit with the magnetic circuit.

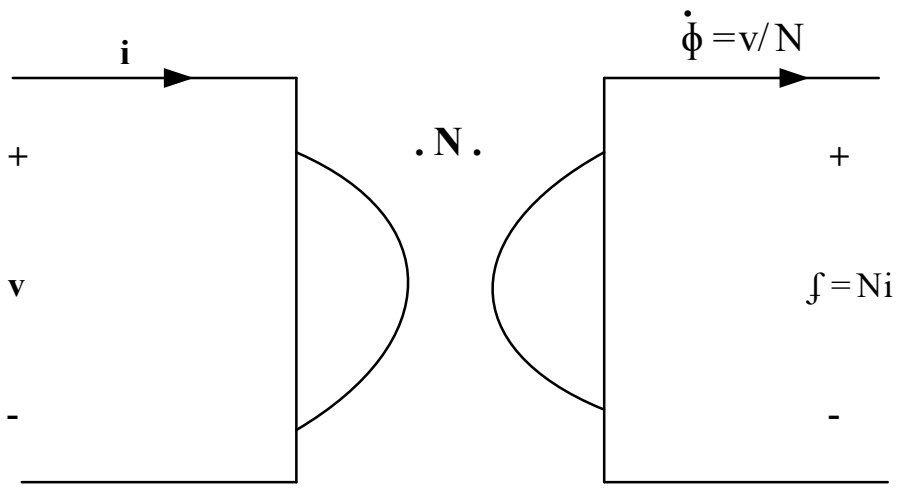


Figure 3.1.4: Gyrator link.

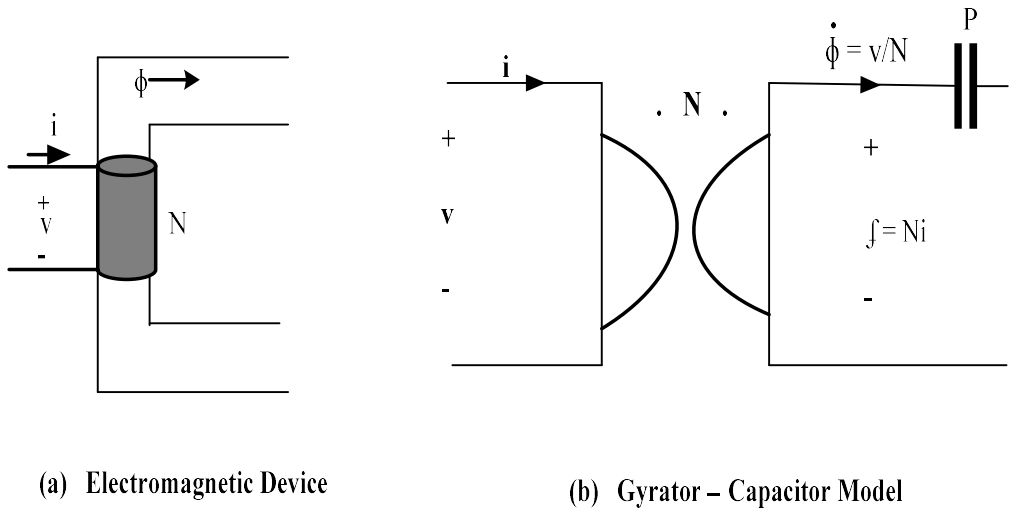
Application of the gyrator to a permeance-capacitance element achieves a gyrator-capacitor model that couples electric and magnetic circuits [17,18,19,20]. The model operates in accordance with the system of equations described in Equation (3.12),

$$\begin{bmatrix} v \\ \int \end{bmatrix} = \begin{bmatrix} 0 & N \\ N & 0 \end{bmatrix} \begin{bmatrix} i \\ \acute{\phi} \end{bmatrix} \quad \text{(3.12)}$$

Where: v is the terminal voltage (V), i is the terminal current (A), $\int$ is the mmf (A · turns), $\dot{\phi}$ is the flux rate (Wb/s) or (V.A. turns) and N is the number of turns.

In Equation (3.12), constant of proportionality, N, represents the turns of the winding which cancels with the turns in the magnetic flow variable to make the units of both flow variables in VA. The gyrator-capacitor model for magnetic circuit modeling is schematically shown in Figure 3.1.5. The gyrator-capacitor model is used to estimate a random magnetic circuit, which makes it possible to model the non-linearity of ferromagnetic core with an application of variable capacitors or variable permeance as illustrated, in Figure 3.1.6.

To model a variable permeance or variable capacitor in P-SPICE, an equivalent permeance needs to be calculated using equation and date table [21,22]. To estimate an equivalent permeance, an ideal transformer model is used [23], by reflecting a unity permeance on the secondary side with respect to primary using a scaling factor k_n as shown in Figure 3.1.7.



(a) Electromagnetic Device (b) Gyrator – Capacitor Model

Figure 3.1.5: Gyrator-capacitor model for magnetic circuit modelling.

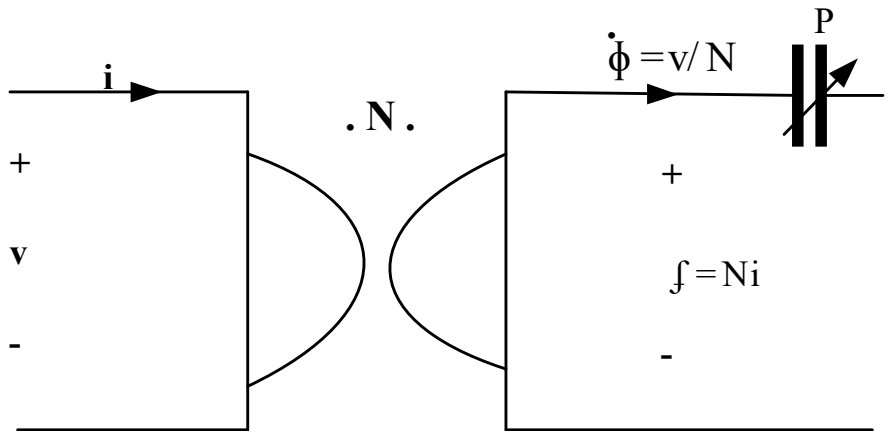


Figure 3.1.6 : Gyrator-capacitor model with variable permeance.

Figure 3.1.7 consists of a dependent voltage source on the primary side and a dependent current source on the secondary side. The use of permeance (P=1) on the secondary side makes the equivalent permeance (P_{eq}) inversely proportional to scaling factor (k_n) and is expressed mathematically as

$$Peq = {}^{1}/_{kn} \quad \text{.....(3.13)}$$

For a non-linear core magnetic circuit, the equivalent permeance can be expressed as the ratio of flux (ϕ) to magneto-motive force (∫) and mathematically is expressed as,

$$Peq = {}^{\Phi}/_{\int} = {}^{\Phi}/_{H.l} \quad \text{.....(3.14)}$$

From Equations (3.13) and (3.14), scaling factor [22] can be calculated as

$$kn = {}^{\{H\left(\frac{\Phi}{A}\right)\}}/_{\Phi} \quad \text{.....(3.15)}$$

Where, H is the magnetic field strength (A/m), B is the magnetic field density (Tesla), A and l are the effective magnetic branch parameters. H(ϕ/A) implies that, magnetic field strength (H) is a function of magnetic field density (B), where B = ϕ/A. In addition, the magnetic field density (B) of the core relates to magnetic field strength (H) as B =μ H. Where, μ represents the permeability which is determined from the B-H curve and represents the non linear magnetic characteristics of the core material.

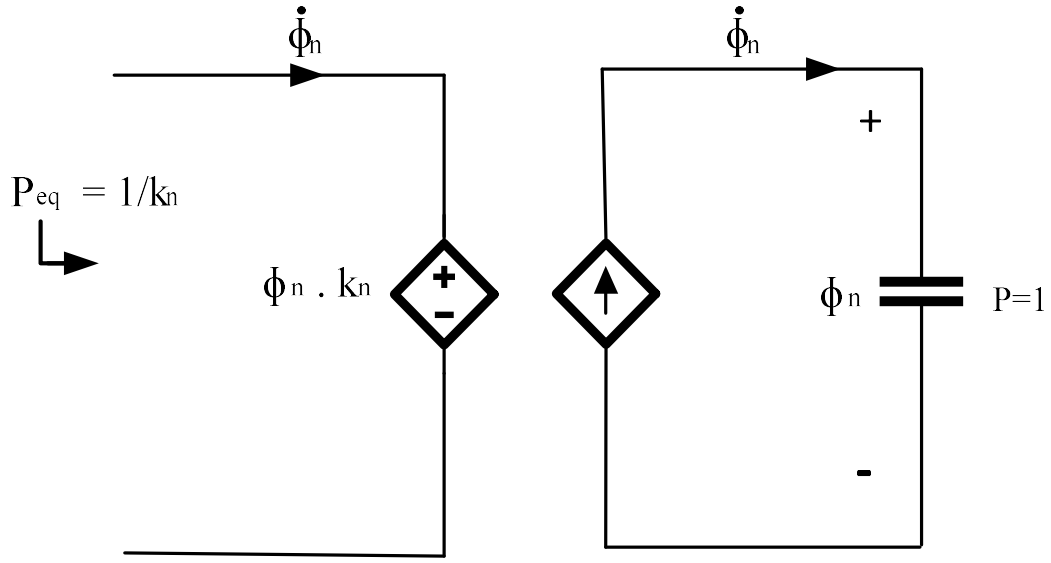


Figure 3.1.7 :Nonlinear permeance (Variable Permeance) application in P-SPICE.

As per electric and magnetic circuit analogy, the electric energy stored in capacitor ($E_{ef} = Q^2/2C$) and the magnetic energy stored in any branch of magnetic circuit ($E_{mmf} = \phi^2 /2P$) imply the following in Table 3.3.

Table 3.3: Analogs of Electric and Magnetic Quantities.

Electric Circuit	Magnetic Circuit
Capacitance (C)	Permeance (P)
Charge (Q)	Flux (ϕ)
Electromotive force (E_{ef}) or the Capacitor voltage (V_c) = Q/C_{eq}	Magnetomotive force(E_{mmf}) = ϕ / P_{eq}

From Table 3.3, it can be concluded that the electromotive force or the voltage applied to a capacitor is equal to the magnetomotive force and therefore, V_c must be equal to ϕ / P_{eq} and from Equation (3.13),(3.14) and (3.15), the input voltage to a transformer from Figure 3.1.7 can be expressed as

$$Vc = \frac{\Phi}{Peq} = \phi \times kn = \left\{H\left(\frac{\Phi}{A}\right)\right\} \times l = \{H(B)\} \times l \quad \text{.....(3.16)}$$

Where, B = ϕ/A.

CHAPTER 4

SINGLE-PHASE TRANSFORMER MODELING USING GYRATOR-CAPACITOR APPROACH

4.1 Single-Phase Transformer Gyrator-Capacitor Model

In this study, gyrator-capacitor approach is used to model the single-phase transformer using P-SPICE [24], an open source analog electronic circuit simulator used for simulation and verification of analog and mixed-signal circuits. The specifications for single-phase transformer are given in the appendix.

The magnetic circuit modeled in this study is represented by four variable permeance blocks, two on each side of the leg of the core and two gyrators to model the two AC windings. DC voltage is applied in the middle to investigate saturation under GIC conditions. It is possible to model the transformer cores exhibiting nonlinear permeability with application tovariable permeances, as shown in Figure 4.1.

P-SPICE does not contain variable permeance (non-linear permeance) capacitor, so variable permeance block for each magnetic branch is made separately in the software using dependent voltage sources [21,25]. The overall constructon for the non-linear permeance or the variable permeance block is composed of two parts with one part showing the schematic for the mmf calculation circuit while the other part estimating the flux. Figure 4.2.1 shows the variable permeance block, obtained from the flux rate and the dependent voltage source. (EVALUE) in (a) block converts the flux to magnetic field density, B by dividing it by the cross sectional area.

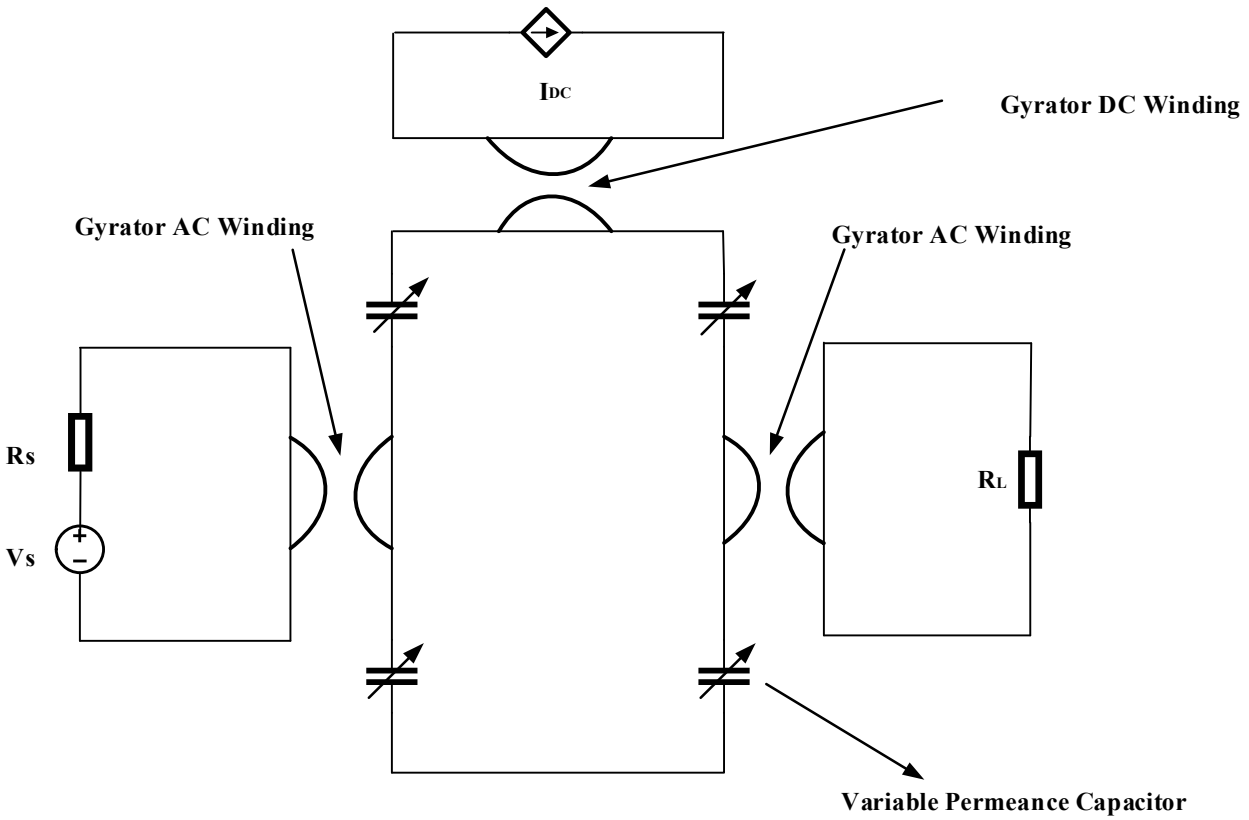


Figure 4.1 : A gyrator-capacitor model with variable permeance for the single-phase winding transformer.

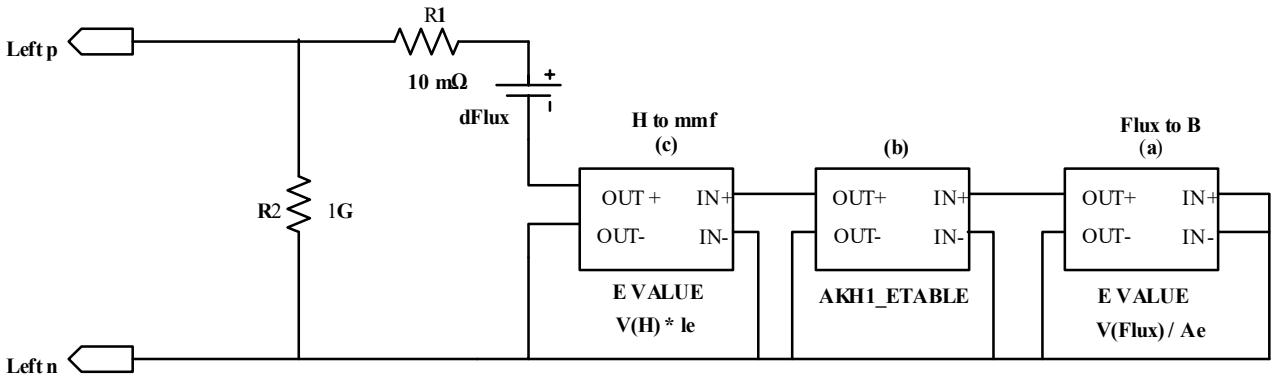


Figure 4.2.1 :Variable permeance block implemented in P-SPICE.

The resulting B is passed to the interpolation element in (b) (ETABLE) for estimation of the magnetic field strength, H. The final step is the conversion of H to magneto-motive force (mmf) by the dependent voltage source (EVALUE), as shown in (c). The second voltage source (EVALUE) samples the voltage (V_H) and mulitplies it by l_e and resulting in the magnetomotive force (mmf).

In addition, the input current to a unity capacitor or permeance is realized by a dependent voltage source GVALUE to calculate flux as shown in Figure 4.2.2. The nonlinear model for variable permeance also consists of extra resistances R1, R2 and R3 to nullify the convergence problem in P-SPICE. Connection of voltage source to a node is provided by R1 while R3 provides the path to ground and the proper sizing of R1 can help improve the hysteresis behavior of ferromagnetic materials [25,26]. Figure 4.2.3 shows the gyrator-capacitor model of single-phase transformer, where LT, LB, RT, RB are the four quadrants of the core and each quadrant is represented by a variable permeance block that includes magnetic characteristic of the core material (AKH1 steel), as shown in the appendix attached.

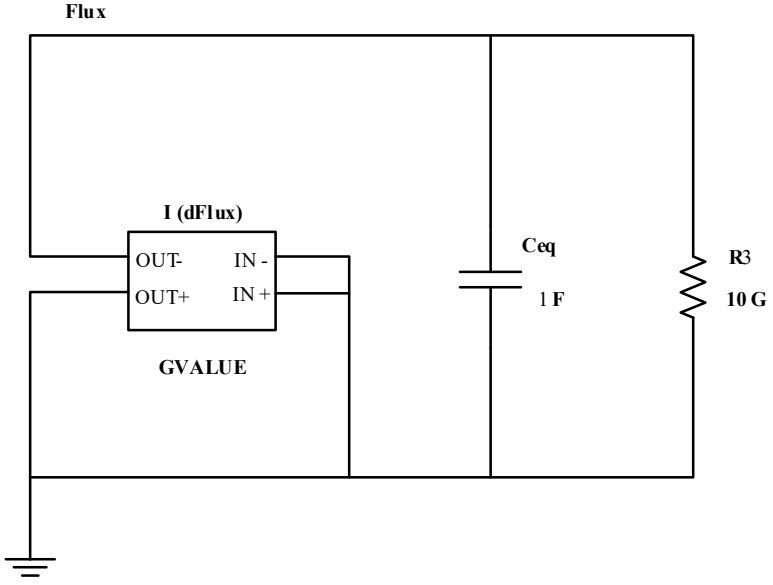


Figure 4.2.2 : Flux calculation circuit in P-SPICE.

The quadrants LT and LB are connected through the primary AC winding of the gyrator using a primary side electric circuit and the quadrants RT and RB are connected through the secondary AC winding of the gyrator using secondary side electric circuit.

The primary side electric circuit is implemented using a source impedance (R_s) and the secondary side electric circuit is implemented using a load impedance (R_L) as shown in Figure 4.2.4. The source impedance R_s plays a very important role in modeling the application of GIC (DC) to a single-phase transformer which is discussed in Chapter 5.

The model also includes the gyrator DC winding and is connected between the quadrant LT and RT using DC circuit. The DC circuit is driven by GIC (DC Bias) current source as shown in Figure 4.2.5. The voltage induced in the AC flux results in the back emf on to the DC winding and the model solves for the back emf as the difference between the flux rate of change of the left and right legs and is given below in the equation. The back emf does not affect the AC system directly but it signifies the design of DC power supply and can be expressed as,

$$EMF = \left(\frac{d\Phi}{dt}\text{left} - \frac{\text{d}\phi}{\text{dt}}\text{right}\right).\text{Ndc} \quad \text{.....(4.1)}$$

Where, EMF represents the back emf, dϕ/dt left is the flux rate in left leg, dϕ/dt right is the flux rate in right leg, and N_{dc} is the number of turns in the DC bias circuit.

The model also evaluates for the magnetizing current, the exciting current and to measure these currents; the load resistor (R_L) is removed from the secondary side electric circuit (open circuit) as shown in Figure 4.2.6. The magnetizing current waveforms are observed without GIC (DC) and the behavior of the exciting current waveforms are observed with the varying values of GIC (DC). The simulation results are discussed further in Chapter 5.

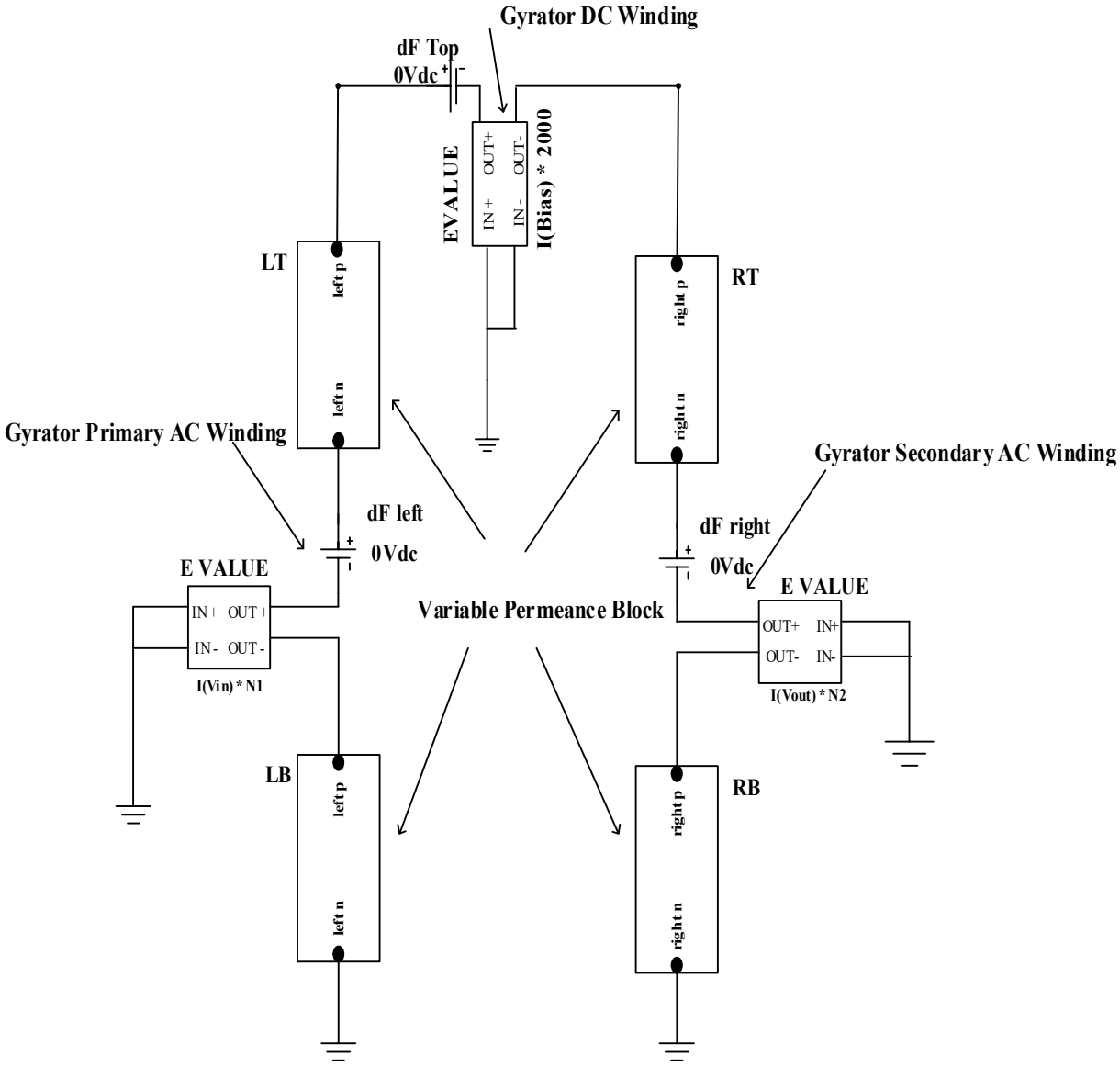
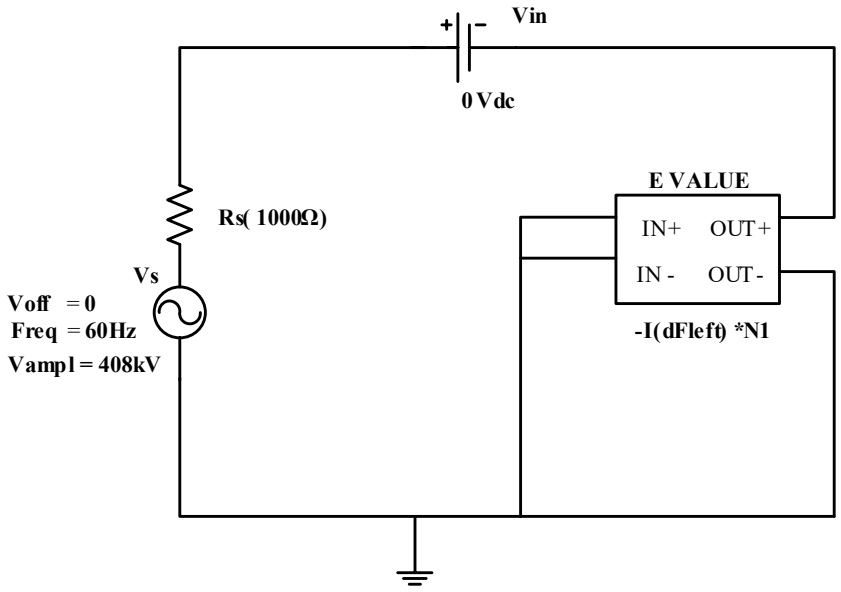
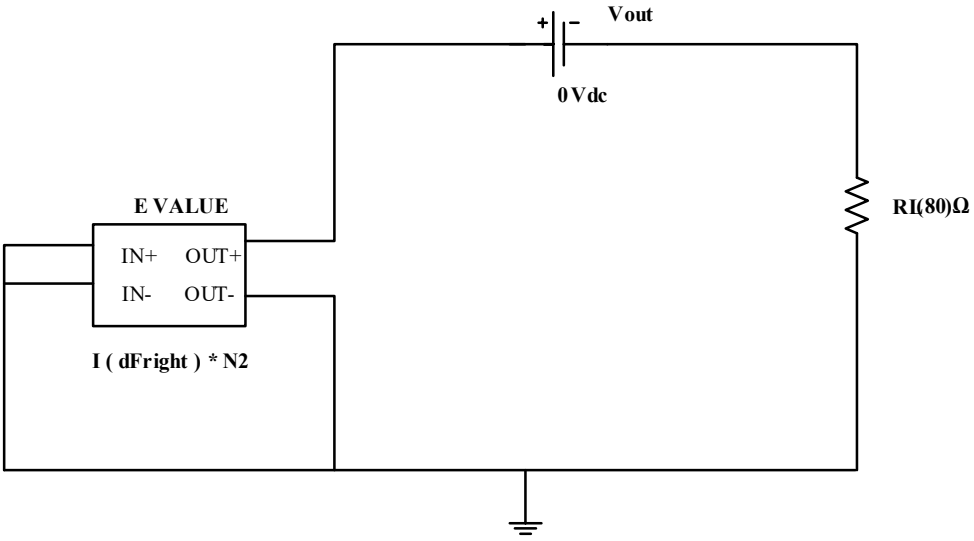


Figure 4.2.3 :Gyrator-capacitor model for two winding core transformer in P-SPICE.



Primary side electric circuit



Secondary side electric circuit

Figure 4.2.4 : AC electric circuits (Primary and Secondary Side) in P-SPICE.

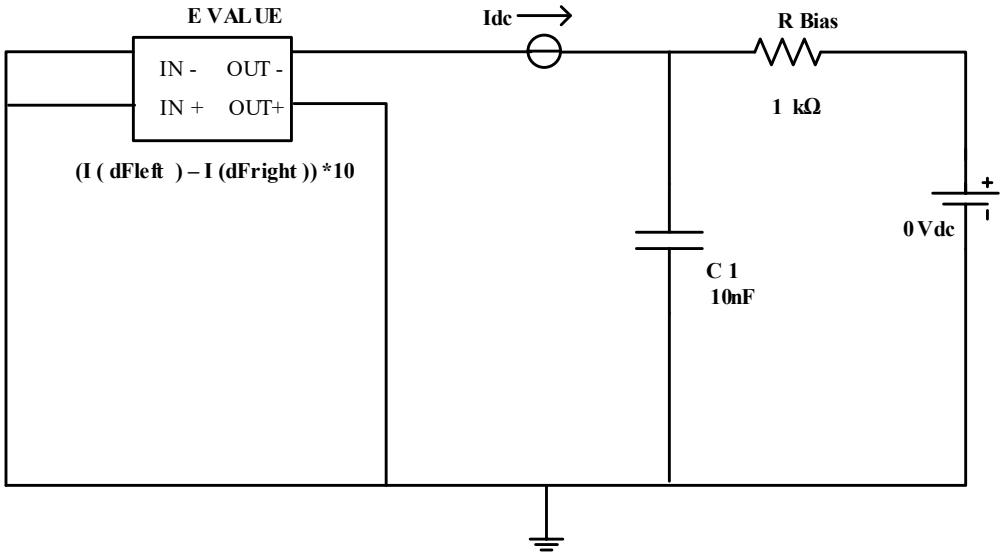


Figure 4.2.5 : DC electric circuit in P-SPICE.

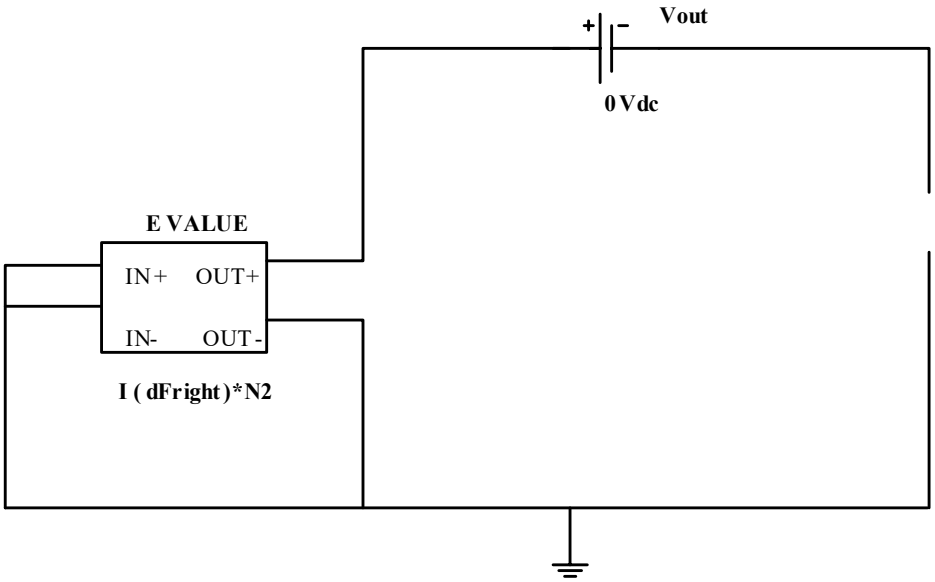


Figure 4.2.6 : AC secondary side electric circuit (Open Circuit) in P-SPICE.

CHAPTER 5

SIMULATION RESULTS

In this chapter, the performance of single-phase transformer is studied using the gyrator-capacitor model. The behavior is observed in the form of simulation results and is divided into two sections as the transformer behavior without GIC (DC) in the circuit and the transformer behavior with GIC (DC). The single-phase transformer is simulated and various parameters such as input/output current, i/o voltages, core flux and exciting current harmonics waveforms resulted from the simulation are achieved. The simulation results show that the source impedance plays a very important role in modeling GIC and therefore, simulations are performed for the above mentioned parameters by chosing different values of the source impedances as low and high impedances.

5.1 Transformer Behavior Without GIC (DC)

The results for the single-phase transformer using the gyrator capacitor model, when no GIC is present are shown in this section. The input/output voltages and current are shown in the Figure 5.1.1 and 5.1.2, when small source impedance is connected in the primary AC circuit and a load resistor (80Ω) is connected in the secondary AC circuit. The same model is then simulated with a large source impedance and the waveforms are obtained for the input/output voltages and currents as shown in Figure 5.1.3 and Figure 5.1.4. This section also validates the induction principle of the transformer as given in the section 2.1 of Chapter 2 for small and large source impedance values.

5.1.1 Input /Output Voltage Waveforms in the Presence of Small Source Impedance

In this sub-section, simulations for input/output voltages are obtained when small source impedance of 4.65 Ω is connected in the primary side AC electric circuit and are shown in the Figure 5.1.1. The following waveforms are obtained from the transient analysis and the input/output voltage of 406kV and 95kV are obtained.

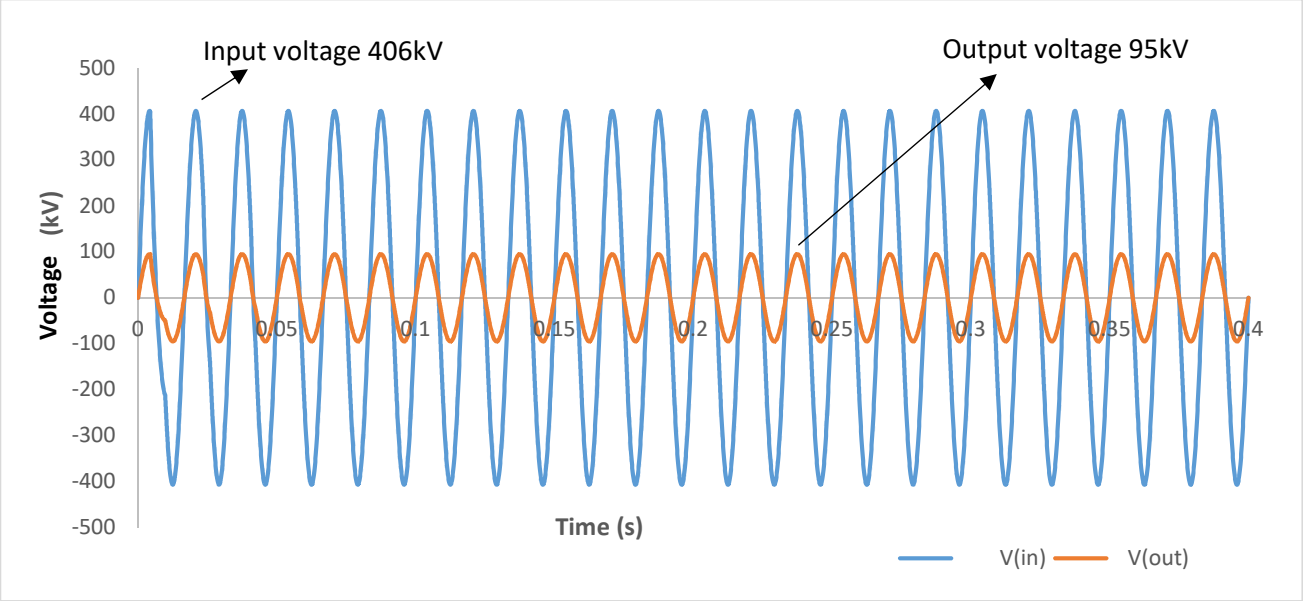


Figure 5.1.1: I/O voltage waveform in the presence of small source impedance.

5.1.2 Input /Output Current Waveform in the Presence of Small Source Impedance

The input/output current simulations are also obtained when a small source impedance is connected in the primary AC winding circuit as shown in Figure 5.1.2.

Observation: From Chapter 2, the induction principle of the transformer states that the voltage ratio, the current ratio and the turns ratio are equal i.e.

$$\frac{Vs(Vout)}{Vp(Vin)} = \frac{Ns}{Np} = \frac{Ip(Iin)}{Is(Iout)} \quad \text{.....(5.1)}$$

It is seen from the Figure 5.1.2 that, in the presence of small source impedance, the spikes result in the current waveforms and therefore, the current ratio can not be determined. However, the voltage and turns ratio are calculated as $\frac{95kV}{406kV} = \frac{56}{240} = 0.23$.

To calculate the current ratio, the same model is simulated using large source impedance (1000Ω) and the voltage and the current waveforms are obtained which verified the induction principle of transformer and are discussed in the next sub-section.

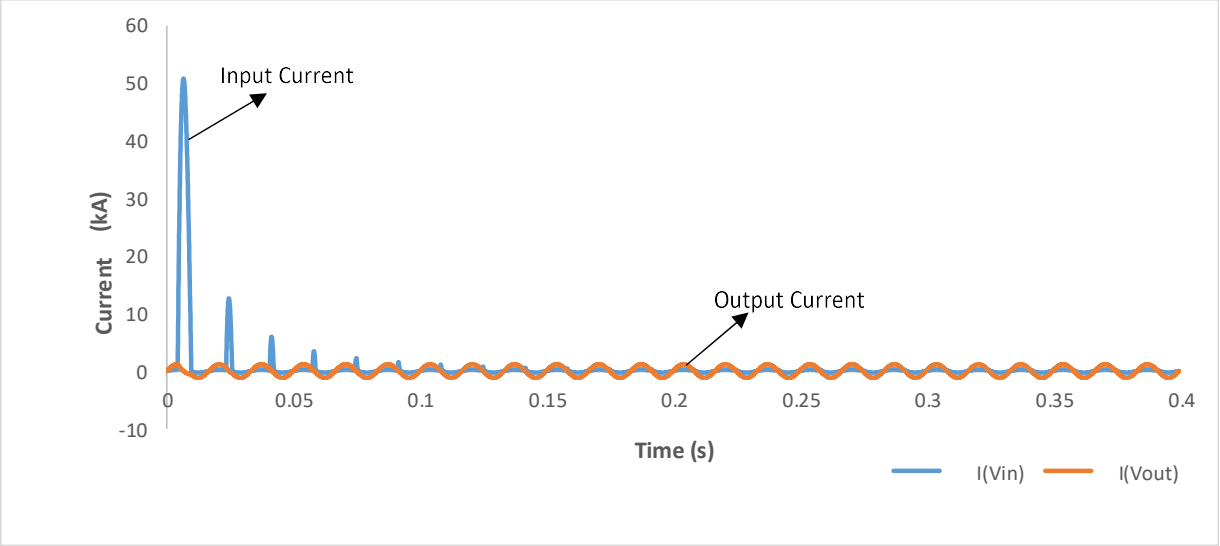


Figure 5.1.2: I/O current waveform in the presence of small source impedance.

5.1.3 Input /Output Voltage Waveform in the Presence of Large Source Impedance

The input/output voltage simulations are obtained when a large source impedance is connected in the primary AC winding circuit as shown in Figure 5.1.3. The following waveforms are obtained from the transient analysis and show the input/output voltage of 242kV and 56kV respectively.

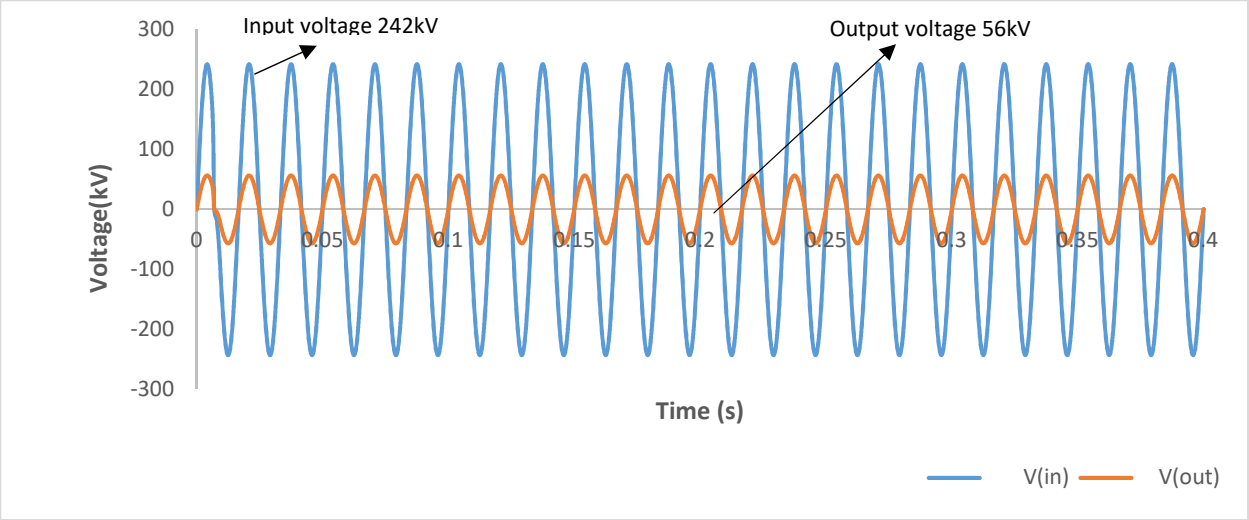


Figure 5.1.3: I/O voltage waveform in the presence of large source impedance.

5.1.4 Input /Output Current Waveform in the Presence of Large Source Impedance

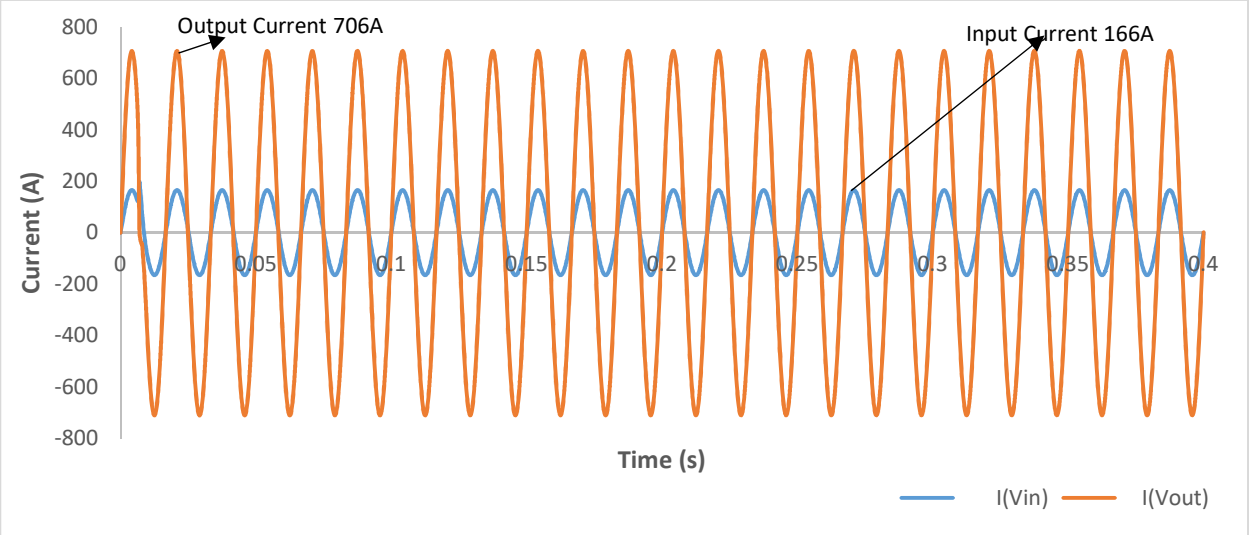


Figure 5.1.4: I/O Current waveform in the presence of large source impedance.

Observation: The input/out put voltages of 242kV and 56kV and input/output currents of 166A and 706A are obtained using large source impedance in the simulation model. Therefore, the current ratio can also be determined as the current flowing in the primary winding ($I_{(Vin)}$) is free from spikes and is a pure sinusoidal wave. The induction principle of transformer is also validated and all the ratios are equal to each other as shown below.

$$\frac{Vs(Vout)}{Vp(Vin)} = \frac{Ns}{Np} = \frac{Ip(Iin)}{Is(Iou\ )} \text{.....(5.2)}$$

$$\frac{56kV}{242kV} = \frac{56}{240} = \frac{166A}{706A} = 0.23 \text{.....(5.3)}$$

As it is clear from the above discussion that a large source impedance value validates the proper transformer induction principle .Therefore, in the next sub-sections and in Section (5.2) the waveforms for flux and the magnetizing current are obtained using large source impedance value.

5.1.5 Flux Waveform

The waveform in Figure 5.1.5 shows the flux waveform for the core of the single-phase winding transformer when no GIC (DC) is present. The flux waveforms for the left and the right legs are overlapping with each other and thus are in phase with each other. However, there appears to be an offset in the fluxes as there is a large time constant associated with the simulation. Ideally, all of the flux measurements in the core should overlap. Figure 5.1.6, shows the simulation results for magnetizing current in the absence of GIC (DC). In saturation mode, the magnetizing current is no longer sinusoidal and has large current peaks and the next section discusses the behavior of single phase transformer in presence of GIC(DC) by using large source impedance.

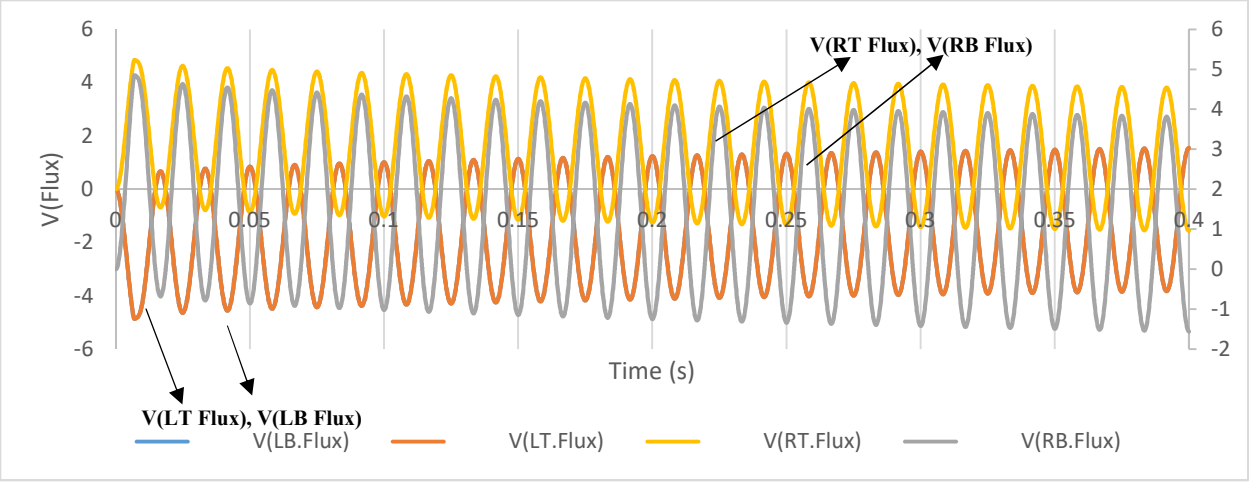


Figure 5.1.5: Flux waveform in the presence of large source impedance without GIC(DC).

5.1.6 Magnetizing Current Waveform

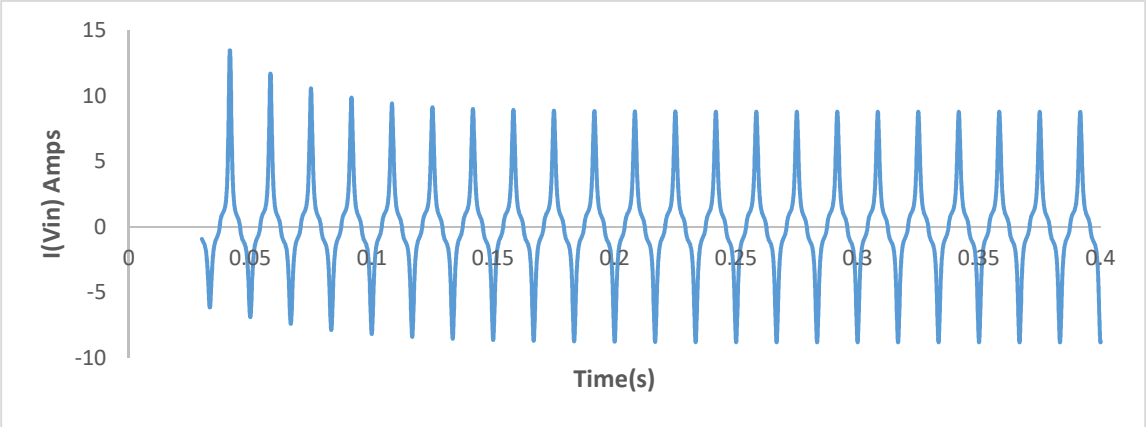


Figure 5.1.6: Magnetizing waveform in the presence of large source impedance without GIC(DC).

5.2 Transformer Behavior With GIC(DC)

In this section, the performance of single-phase transformer is discussed in the presence of GIC(DC). As explained earlier, during a geomagnetic event, GIC is injected into the grounded neutral of the transformers. These GIC are effectively DC current that cause a DC offset flux in the core. This in turn, causes half cycle saturation of the flux in the core which results in harmonics currents and heating issues within the affected transformer. The half-cycle saturation of the flux in the core is discussed in this section.

5.2.1 Flux Waveform

The waveforms obtained in this sub-section shows the behavior of flux in the core in the presence of GIC , and the simulation results obtained shows that the flux of the core is saturated at high value of GIC(DC). The simulations are seen for different magnitudes of GIC (DC) i.e. 10A,100A,300A,500A and 700A. It can be noted that in Figure 5.2.1.1, there is a time constant associated with the simulation, but the transient settles after 200ms (0.2s) . The resulting core flux measurements are offset in proportion to the applied DC flux. Figure 5.2.1.1 shows the flux waveforms when DC current starts building up and the core starts saturating because of the saturation in flux. Figure 5.2.1.2 shows the behavior of the core when the magnitude of the DC current increases and the fluxes in the left and the right legs are moving apart. Figure 5.2.1.3 and Figure 5.2.1.4 shows that the fluxes in the left and the right leg are finally separated and are entered in saturation as shown in Figure 5.2.1.5.

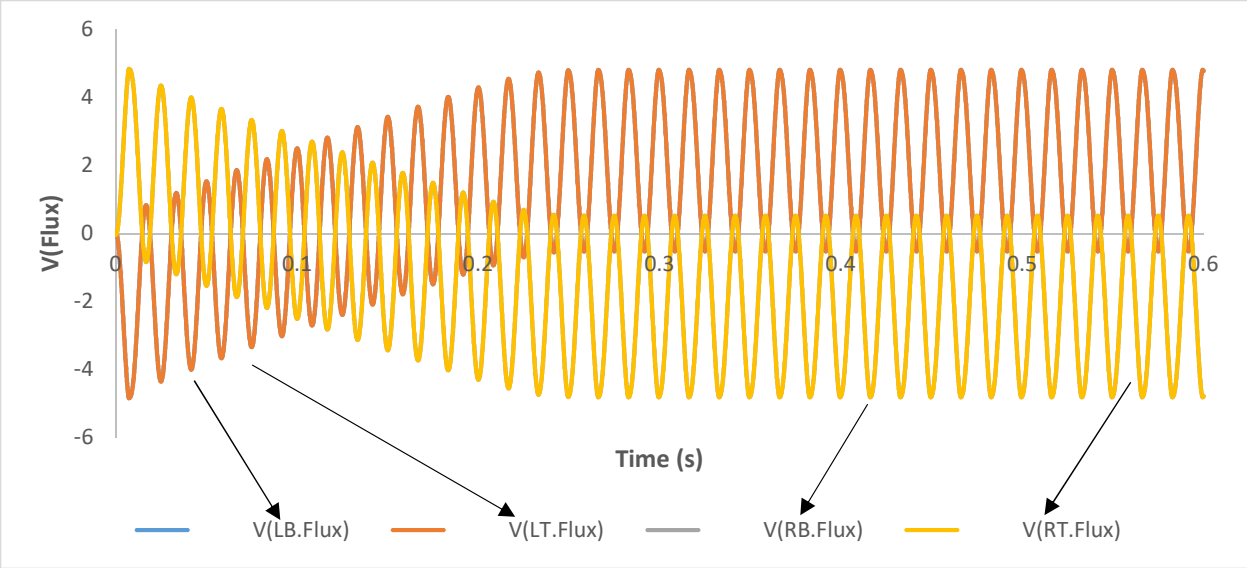


Figure 5.2.1.1: Flux waveform for 10A GIC(DC) in the presence of large source impedance.

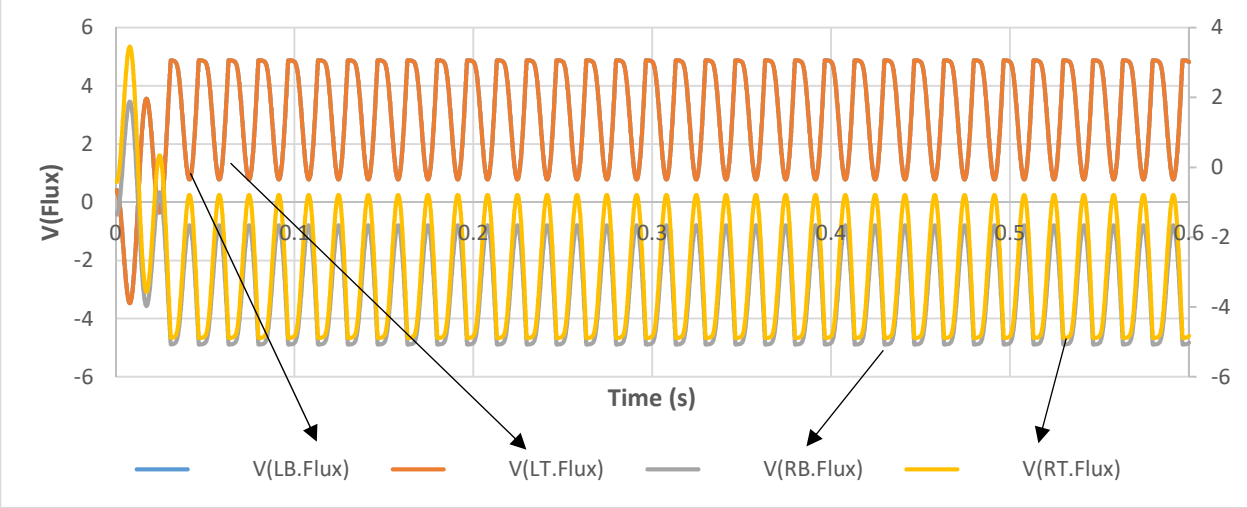


Figure 5.2.1.2: Flux waveform for 100A GIC(DC) in the presence of large source impedance.

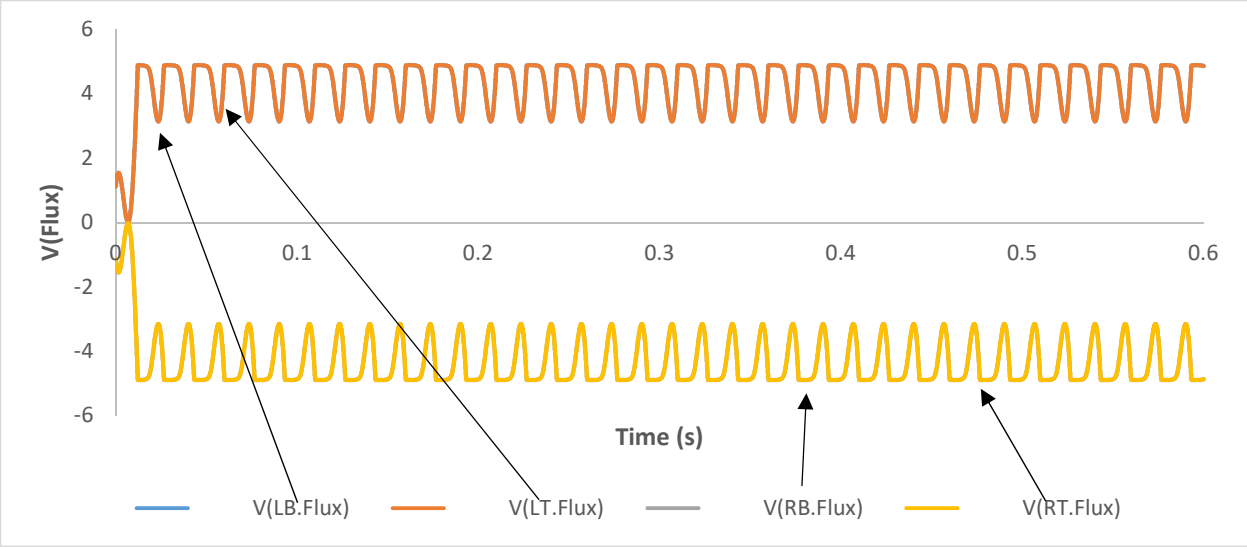


Figure 5.2.1.3: Flux waveform for 300A GIC(DC) in the presence of large source impedance.

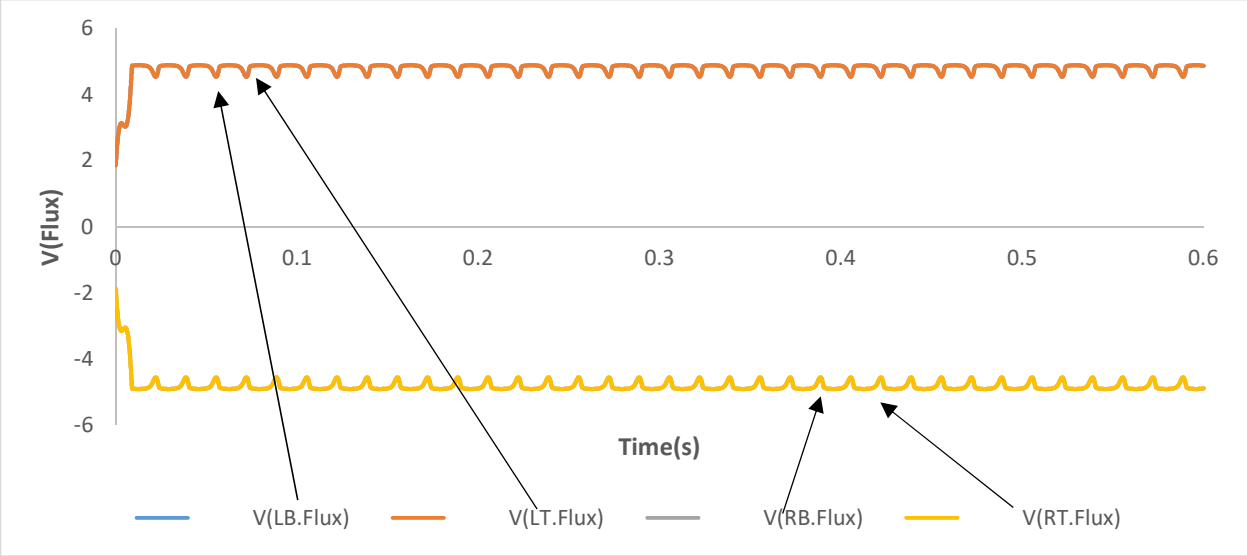


Figure 5.2.1.4: Flux waveform for 500A GIC(DC) in the presence of large source impedance.

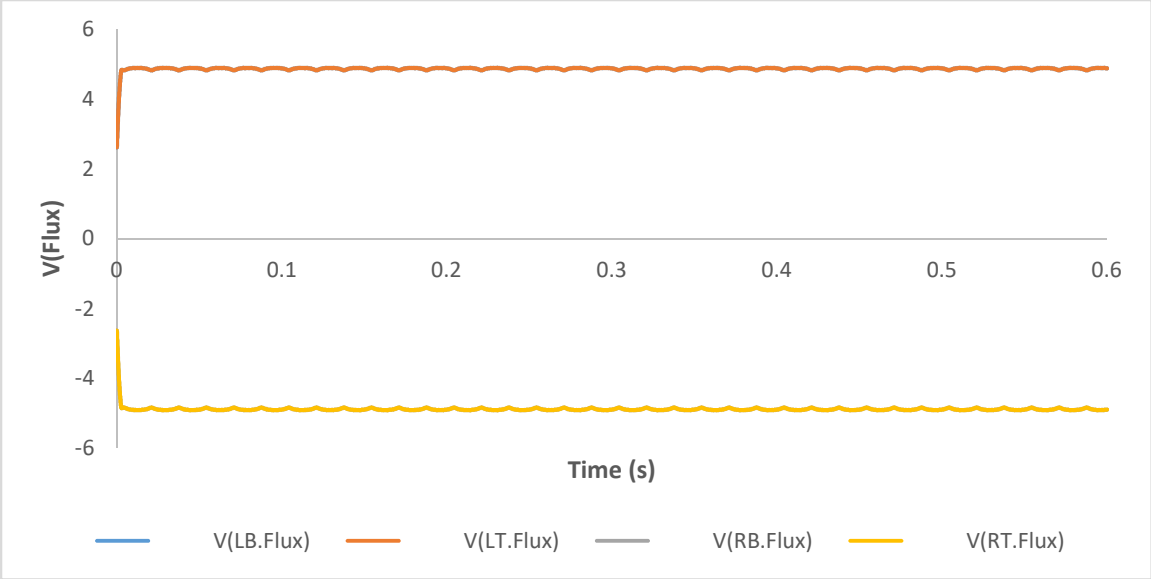


Figure 5.2.1.5: Flux waveform for 700A GIC(DC) in the presence of large source impedance.

5.2.2 Exciting Current Waveform

The purpose of this sub-section is to look for the exciting current waveform for single phase transformer using the gyrator-capacitor model. The model is simulated to obtain the exciting current in the presence of GIC and the behavior is observed with lower to higher magnitude of GIC. To explore the similar behavior as reported in [13] for exciting current as shown in Figure 5.2.2.1, the simulation setting window in the simulation software is set to start saving data after 30ms (0.03s) in the transient analysis.Figure 5.2.2.2 shows the waveform for exciting current when the magnitude of GIC is low e.g. 10A and after that the magnitude of GIC is increased and the exciting current waveform behavior is again observed and recorded upto 400A, in Figure 5.2.2.3 and Figure 5.2.2.4, respectively. Figure 5.2.2.1 shows the simulated exciting current waveform for single-phase core transformer with a GIC of 11.5A, used as a reference for the thesis.

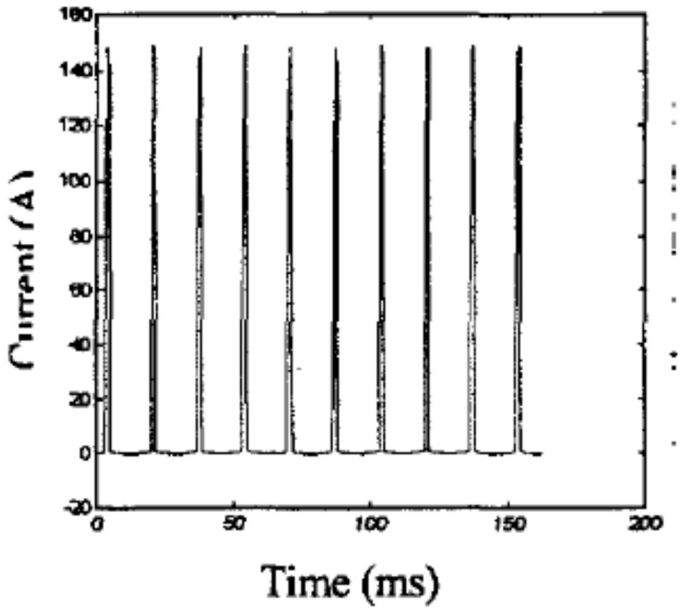


Figure 5.2.2.1: Exciting current waveform for 11.5A GIC(DC)[13].

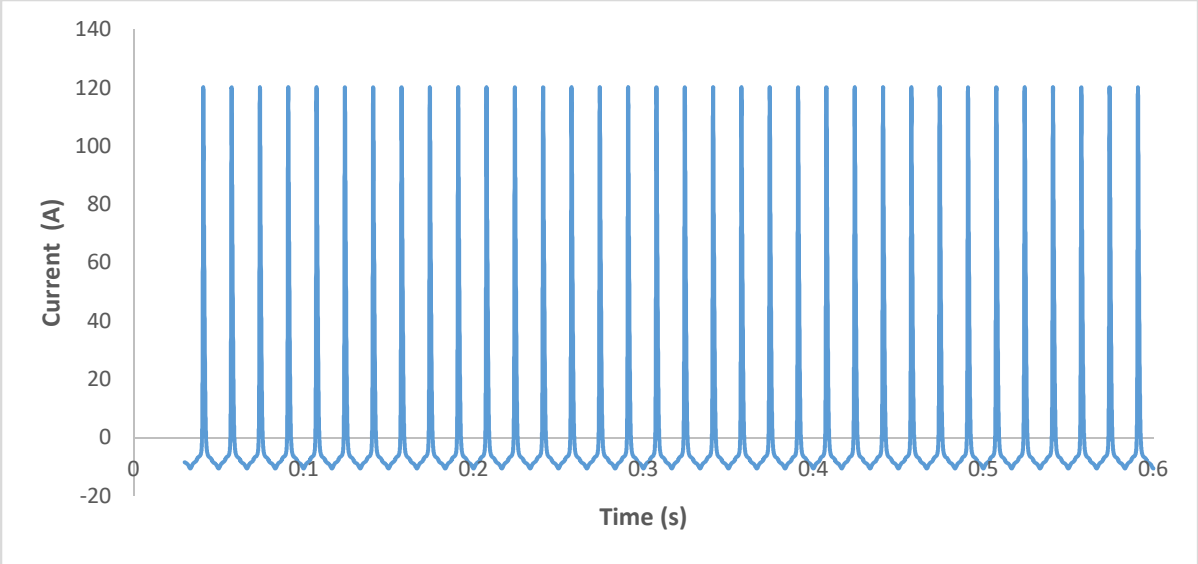


Figure 5.2.2.2: Exciting current waveform for 10A GIC(DC).

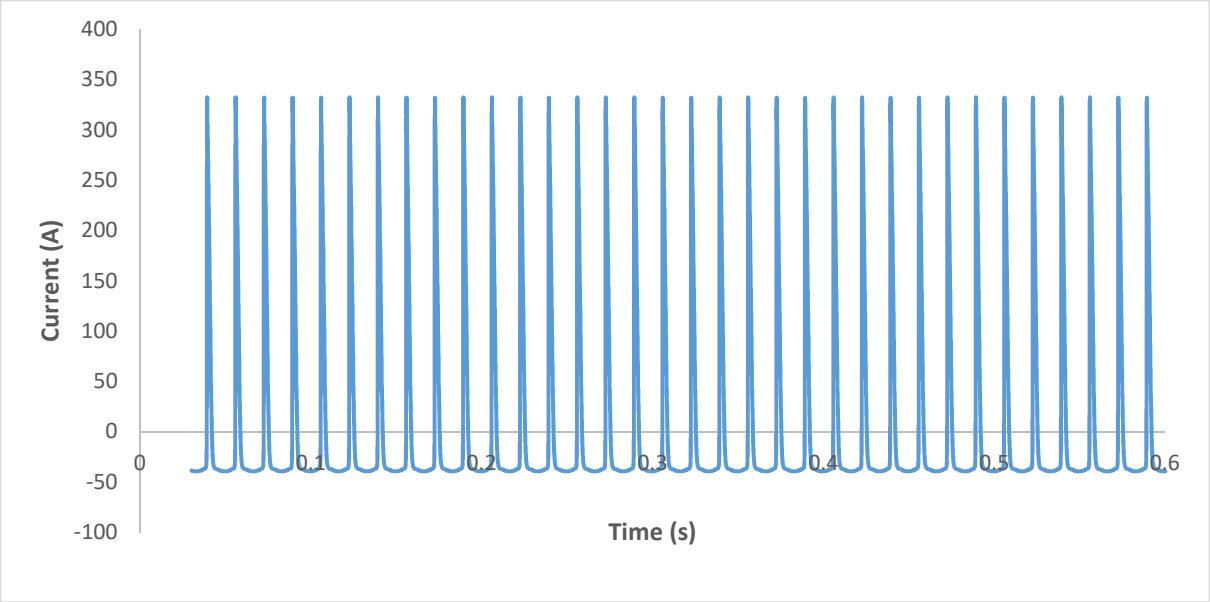


Figure 5.2.2.3: Exciting current waveform for 50A GIC(DC).

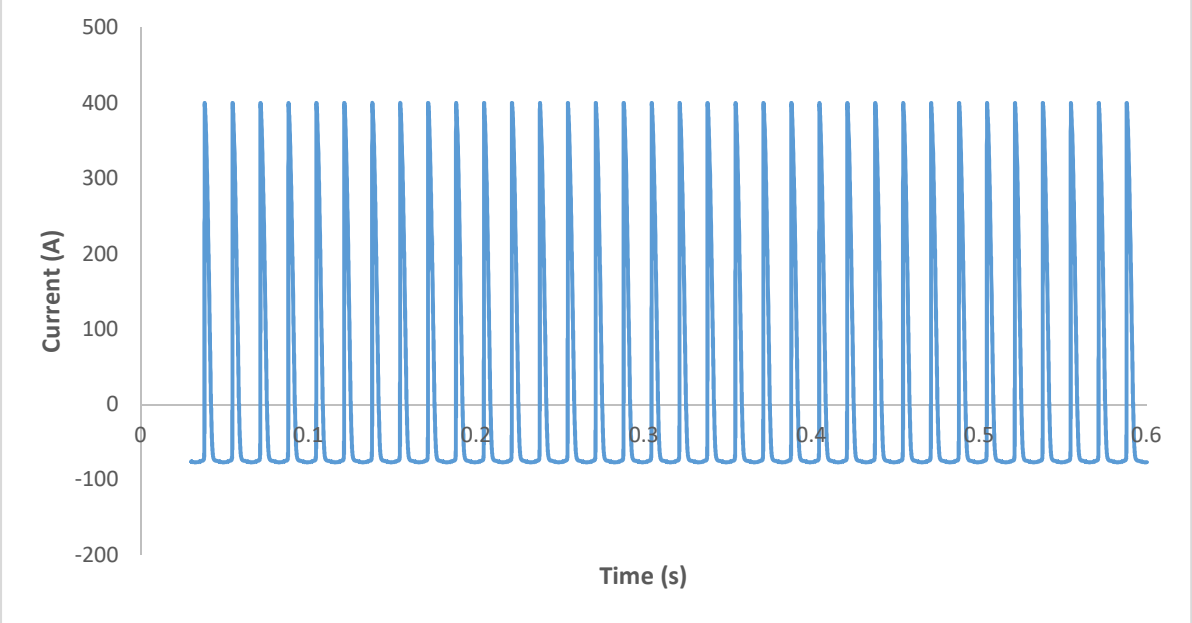


Figure 5.2.2.4: Exciting current waveform for 100A GIC(DC).

5.2.3 Exciting Current Harmonics

The frequency spectrum with a varying GIC (DC) for a single-phase transformer is analyzed in this sub-section. First, the harmonics are obtained, using 10A GIC (DC) as shown in Figure 5.2.3.1 and then the similar results are obtained by using 50A and 100A of GIC (DC) as shown in Figure 5.2.3.2 and Figure 5.2.3.3 respectively. It can be seen that in all the three cases of GIC (DC) , an increase in the frequency leads to a decrease in the amplitude of the current. To verify the harmonics, the waveforms are also compared with the 2001 IEEE paper [13] as shown in Figure 5.2.3.4. The harmonic waveform shows the similar behavior, which shows that the amplitude of the current is decreasing with increase in the frequency. To look for the level of the distortion present in the system, total harmonic distortion is also calculated for 10A GIC (DC) in the simulation environment (P-SPICE) and is attached in the Appendix.

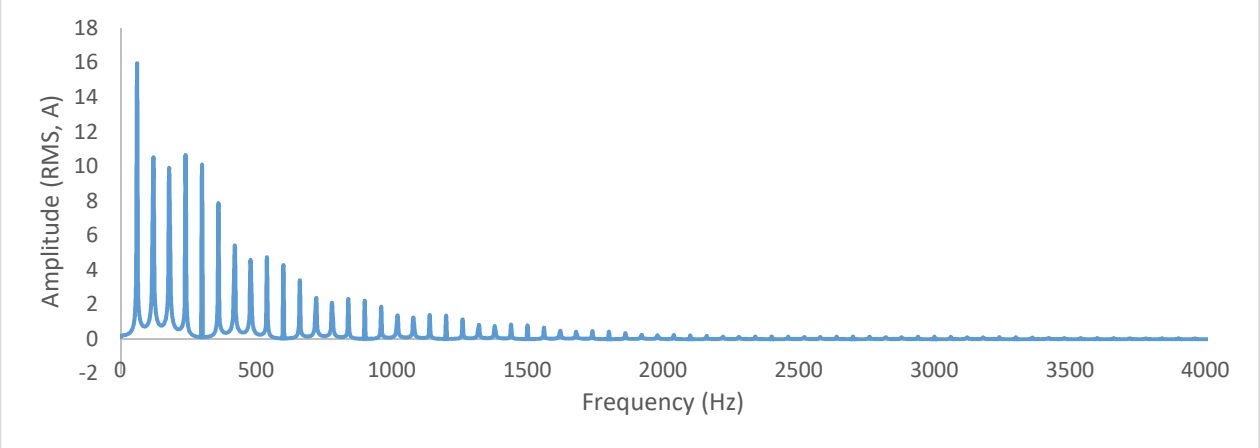


Figure 5.2.3.1: Exciting current harmonics for 10A GIC(DC).

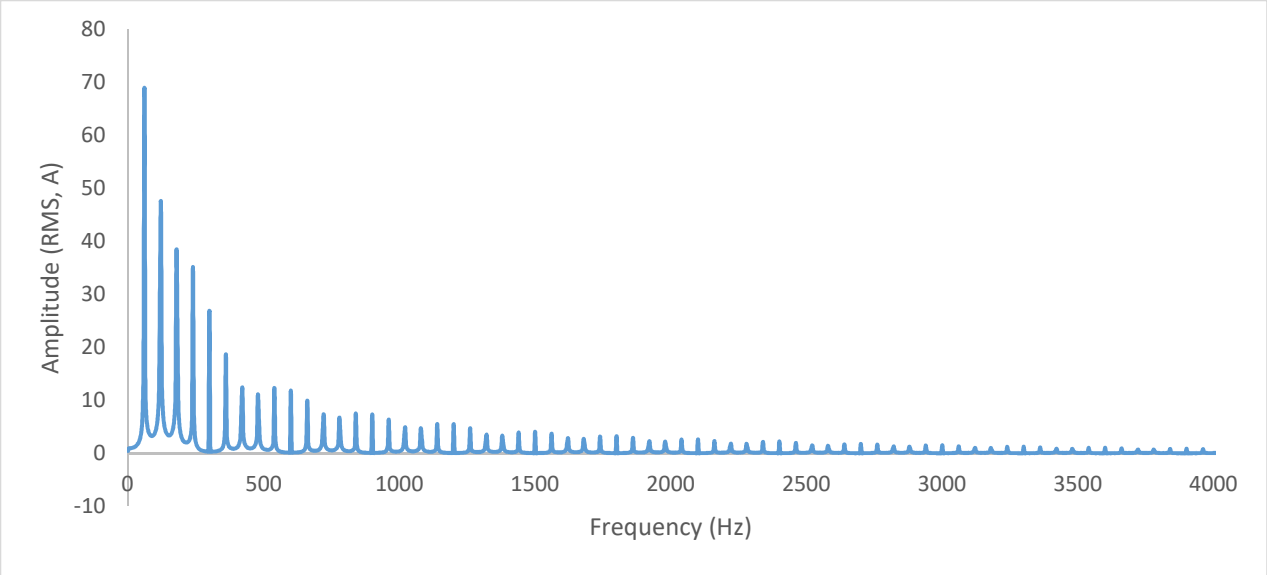


Figure 5.2.3.2: Exciting current harmonics for 50A GIC(DC).

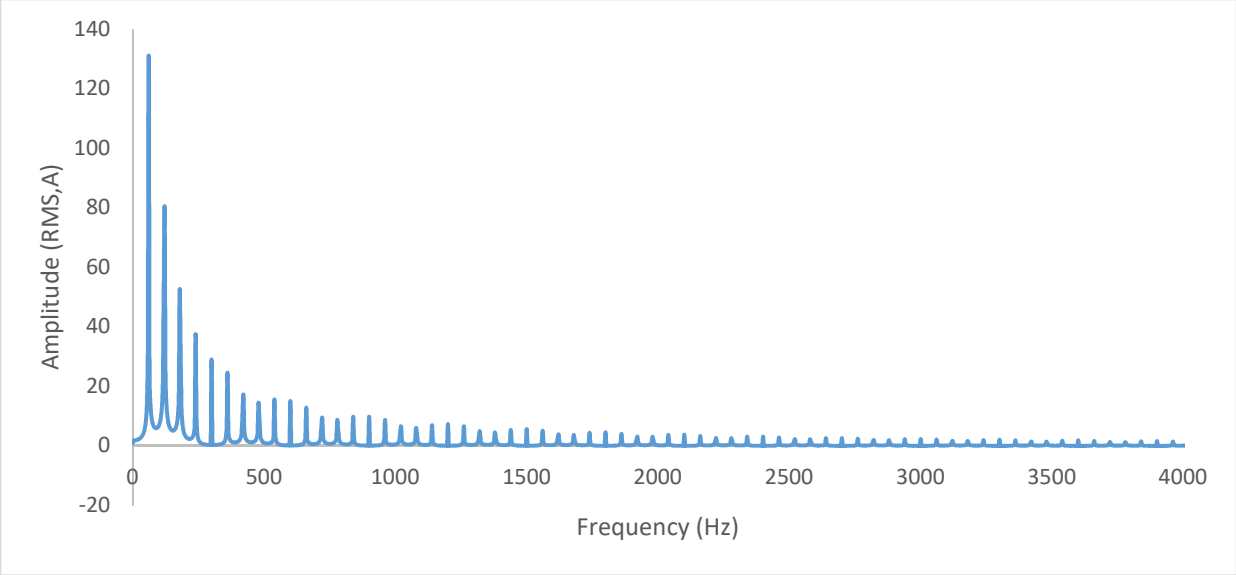


Figure 5.2.3.3: Exciting current harmonics for 100A GIC(DC).

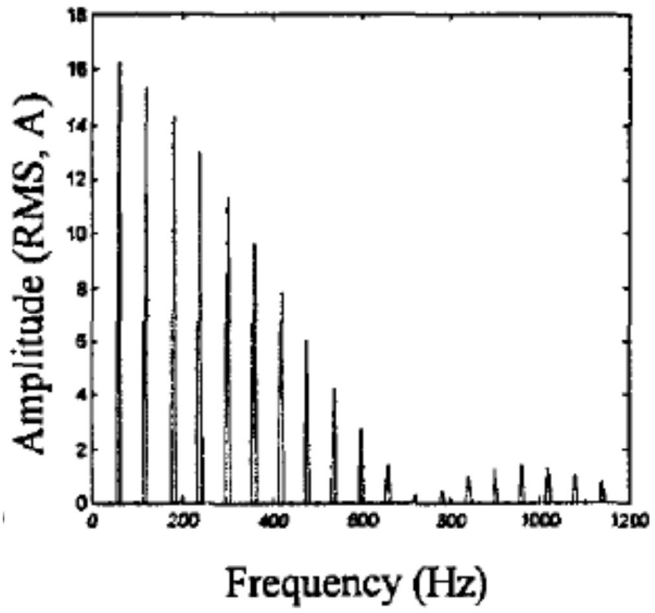


Figure 5.2.3.4: Exciting current harmonics for 11.5A GIC(DC) [13].

5.2.4 Output Waveform

This sub-section shows the resulting wave forms for output current in saturation when different magnitude of GIC current flows in the circuit. The small magnitude of GIC does not affect the output current while the higher magnitude of currents (greater than equal to 50A) affect the output current as shown in the Figure 5.2.4.1, Figure 5.2.4.2, Figure 5.2.4.3 and Figure 5.2.4.4, respectively.

In the section 5.2, the behavior of single-phase transformer using the gyrator-capacitor model is discussed in the presence of GIC (DC). As discussed earlier, when GIC flows in the transformer , the flux in the core gets saturated. The behavior is observed by looking at various waveforms such as flux, exciting current, harmonics and output with different magnitudes of GIC. On the basis of these waveforms, the conclusion and future scope is given in the next chapter.

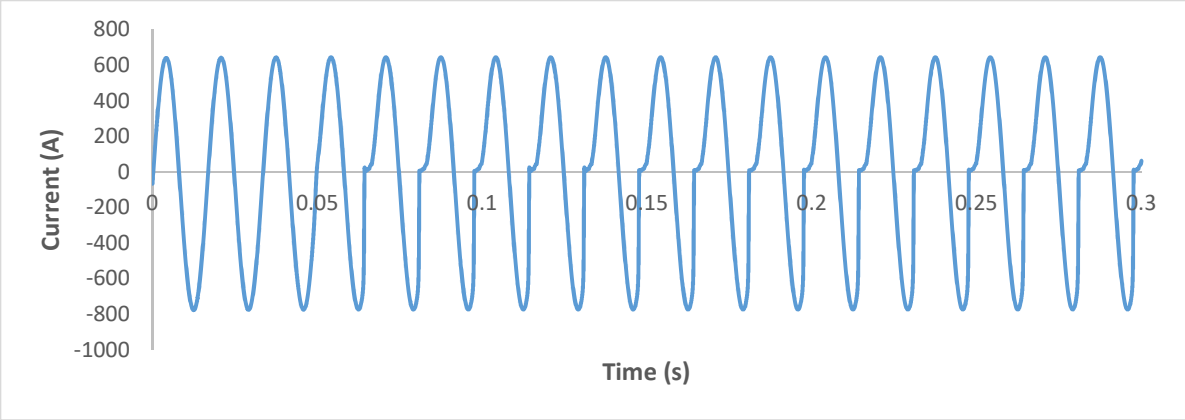


Figure 5.2.4.1: Output waveform for 50A GIC(DC).

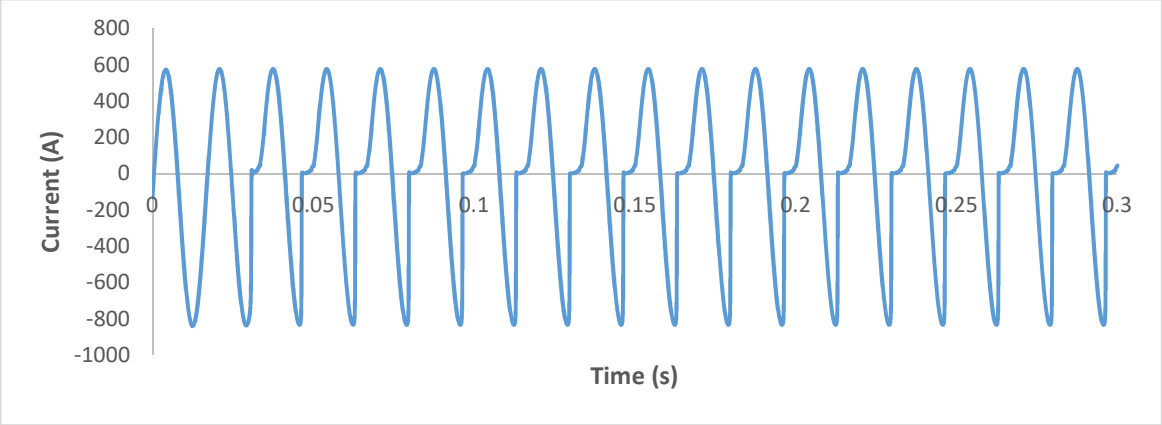


Figure 5.2.4.2: Output waveform for 100A GIC(DC).

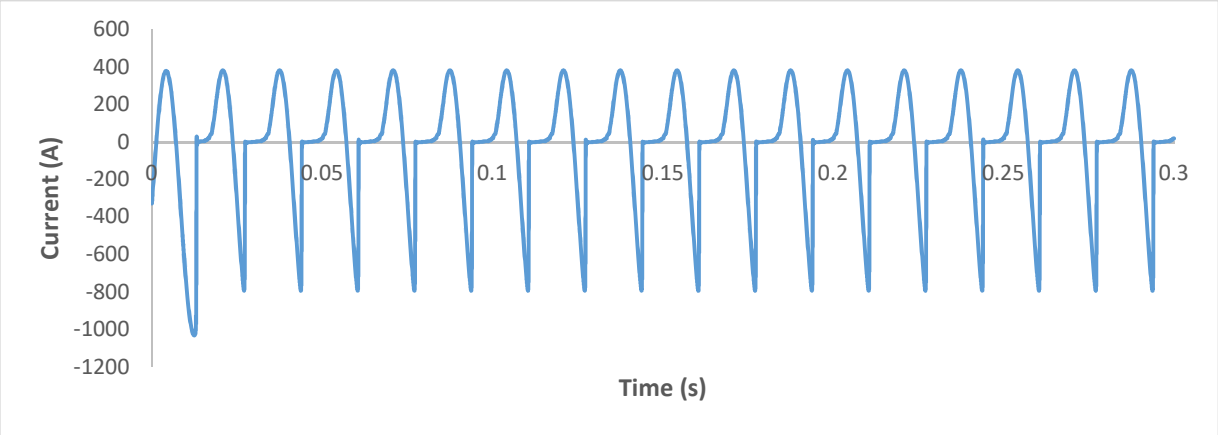


Figure 5.2.4.3: Output waveform for 250A GIC(DC).

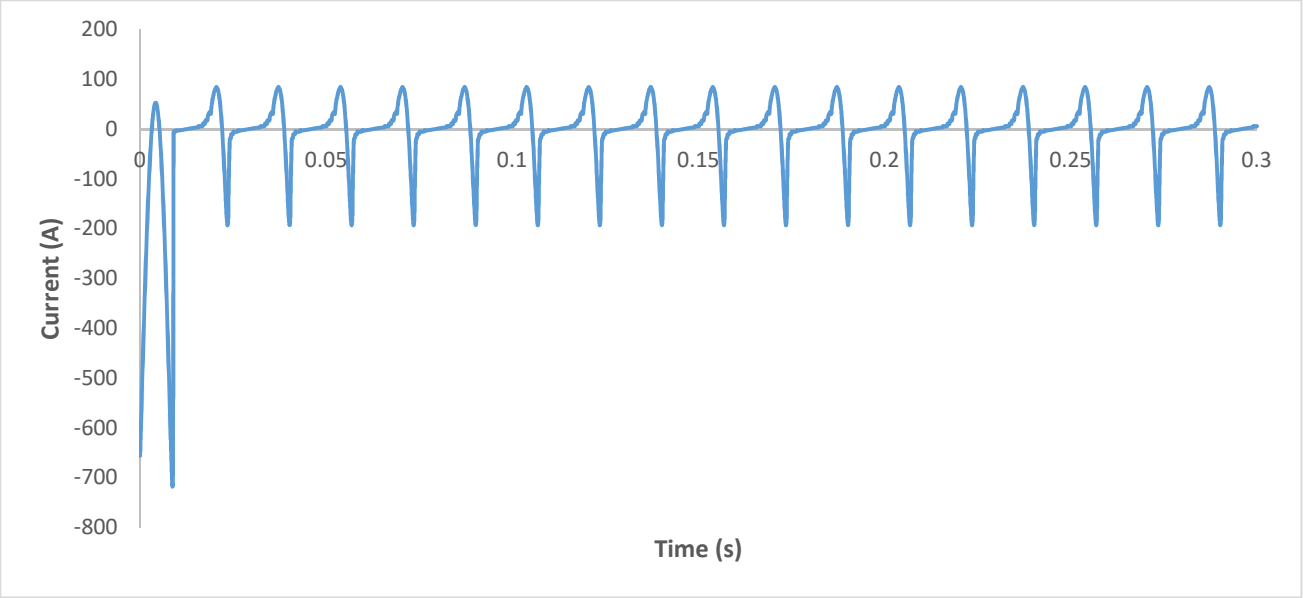


Figure 5.2.4.4: Output waveform for 500A GIC(DC).

CHAPTER 6

CONCLUSIONS AND FUTURE WORK

This thesis describes the development of the gyrator-capacitor model to represent the behavior of a single-phase transformer under geomagnetically induced current (GIC) conditions. The gyrator acts as an interface that couples the electric and magnetic circuits, making it possible to simulate simultaneously and the capacitor models the flux path in the core. The gyrator-capacitor method has an advantage of representing the flux in each leg of the core and the back emf on DC winding. A simple core single-phase transformer is modeled using P-SPICE software tool and simulations are achieved. The behavior of the model seems to be dependent on the source impedance of the electrical circuit. When using a small source impedance, the model does not exhibit the behavior expected by a transformer under GIC. However, by increasing the source impedance the model was able to achieve some positive results and the core flux would offset in proportion to the DC source setting. When the DC current was set large enough the flux experienced half-cycle saturation, which is the expected behavior of a transformer core under GIC conditions. However, the increased source impedance resulted in simulation transients with large time constants. In future , more work is necessary to determine why the source impedance has such a large effect on model behavior.

REFERENCES

1. “North American Electric Reliability Corporation GMD Task Force, Effects of Geomagnetic Disturbances on Bulk Power Systems,” Special Reliability Assessment Interim Report Feb.2012.[Online].Available: http://www.nerc.com/pa/RAPA/ra/Relaibility%20Assessments%20DL/2012GMD.pdf

2. AfshinRezaei-Zare, “Behavior of Single Phase Transformers Under Greomagnetically Induced Current Conditions,” IEEE Transactions on Power Delivery,Vol.29,No.2, April 2014.

3. Luis Marti, AfshinRazaei-Zare,Andrew Yan, “Modeling Considerations for the Hydro One Real- time GMD Management System,” IEEE Power and Energy Society General Meeting (PES)[1944-9925], 2013.

4. D.H.Boteler,L.Trichtchenko,R.Pirjola,J.Parmelee,S.Souksaly, A.Foss,andL.Marti, “Real time Simulation of Geomagneticlly Induced Current.” Canada, Ottawa. 2007. 7th International Symposium on Electromagnetic Compatibility and Electromagnetc Ecology, pg : 261-264.

5. MattiLahtinen, JarmoElovaara, “GIC Occurrences and GIC Test for 400kV System Transformer,” IEEE Transactions on Power Delivery, Vol.17, No.2, April 2002.

6. Philip R. Price, “Geomagnetically Induced Current Effects on Transformers,” IEEE Transactions on Power Delivery. Vol.17, No.4, October 2002.

7. Luis Marti,AfshinRezaei-Zare and ArunNarang, “Simulation of Transformer Hotspot Heating Due to Geomagnetically Induced Current,” IEEE Transactions on Power Delivery , Vol.28, No.1,January 2013.

8. IEEE Guide for Loading Mineral Oil Immersed Transformers, IEEE Standard C57.91-1995,1995.

9. J.A. Patel, R.S.Mehta, S.B. Rathod,K.J. Patel,V.N. Rajput,and K.S. Pandya, “Analysis of Geomagentically Induced Current in Transformer,” International Conference on Electrical, Electronics, and Optimization Tecniques (ICEEOT), 2016.

10. Nobuo Takasu and Tetsuo Oshi, Fumihiko Miyawaki,Sadamu Saito, Yasuo Fujiwara, Japan, “An Experimental Analysis of DC Excitation of Transformer by Geomagnetically Induced Current,” IEEE Transactions on Power Delivery,Vol.9, No.2, April 1994.

11. Shu Lu, Yilu Liu, “A Fundamental Analysis of Transformer GIC Magnetization Using the Finite Element Approach,” Proceedings of the American Power Conference, April 1991, Illinois Inst. Technol. Illinois, USA, pp.1173-1178.

12. R.A. Walling and A.H.Khan, “Characterisitics of Transformer Exciting Current During Geomagnetic Disturbances,” IEEE Power Delivery,Vol.6, No.4, pp.1707-1714, Oct 1991.

13. X.Dong, Y.Liu, and J. Kappenman, “Comparative Analysis of Exciting Current Harmonics and Reactive Power Consumption from GIC saturated Transformers,” in proceeding IEEE Power Energy Society Winter Meeting, Columbus OH, USA, Jan 2001, pp. 318-322.

14. Y. Lee and M.Chow, “Modelling and Teaching of Magnetic Circuits,” Asian Power Electronics Journal, Vol.1, No.1, pp.15-20, 2007.

15. B. Tellegan, “The Gyrator , A New Electric Circuit Element,” Philips Research Reports,Vol.3, pp.81-101,1948.

16. K.M. Adams, E.F. Deprettere and J.O. Voorman, “The Gyrator in Electronic Systems,” Advances in Electronics and Electron Physics, Vol.37, pp. 79-180,1975.

17. R.W. Butenbach, “Analogs Between Magnetic and Electric circuits,” Electronic Products, pp.108-113, October1969.

18. R.W. Butenbach, "Improved Circuit Models for Inductors Wound on Dissipative Magnetic cores," in 2nd Asilomar Conf. on Circuits and Systems, Pacific grove, CA,1968.

19. D.C. Hamill, "Lumped Equivalent Circuits of Magnetic Components: The Gyrator Capacitor Approach," IEEE Transactions On Power Electronics, Vol.8, No.2, pp.97-103,1993.

20. M. Eaton, "Modelling Magnetic Devices Using a Gyrator Re-cap Core model," Northcon/94 Conference Record, Seattle, WA,1994.

21. E.Rozanov and S.Ben-Yaakov, "Analysis of Current Controlled Inductors by New SPICE Behavioral Model," HAIT Journal of Science and Engineering B, Vol.2, No. 3-4, pp. 558-570, 2005.

22. E. Rozanov and B. Ben -Yaakov, "A Spice Behavioral Model for Current Controlled Magnetic Inductors," in Electrical and Electronics Engineers in Israel,2004. Proceedings, 2004 23rd IEEE Convention of 2004.

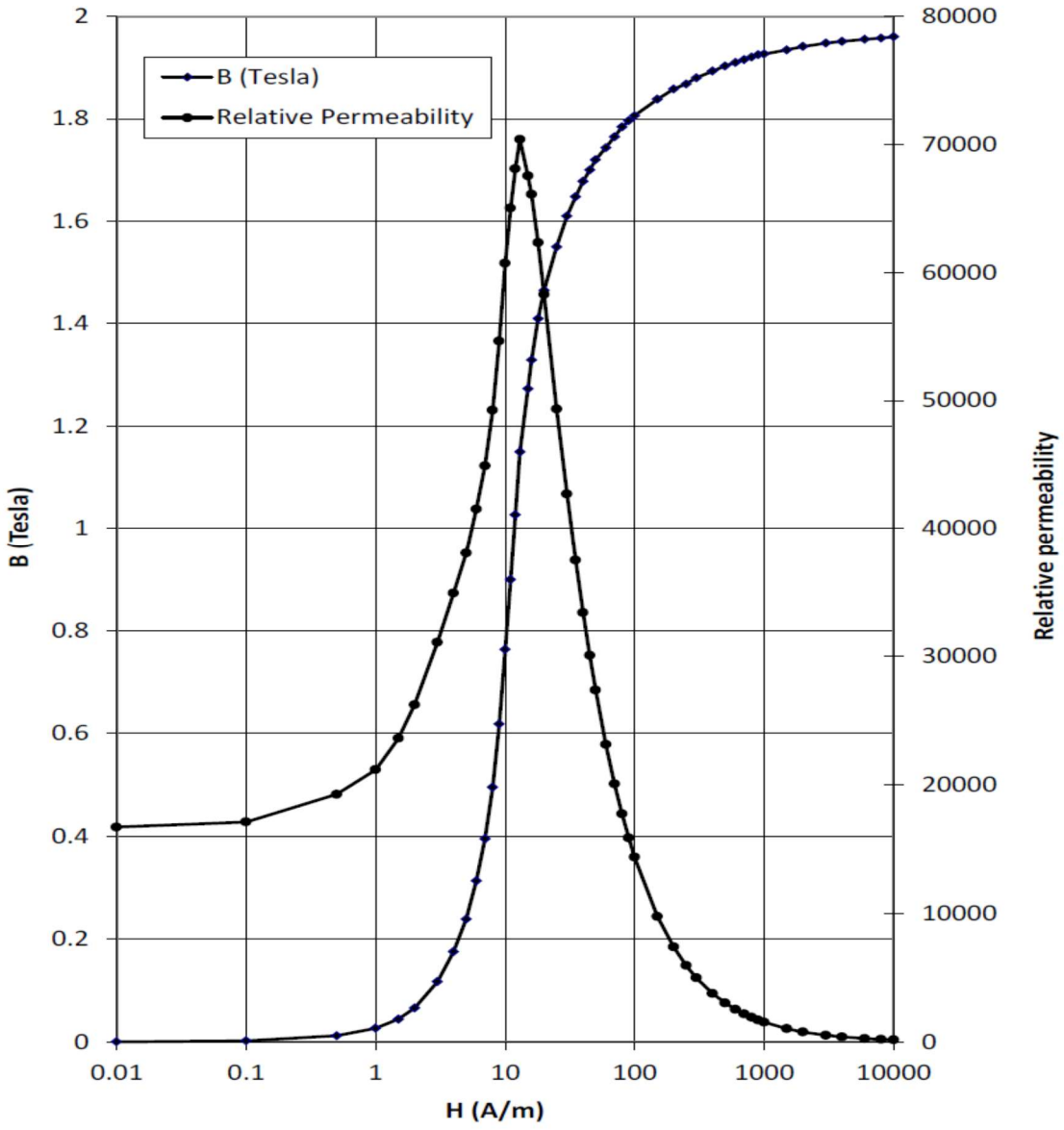
23. R. King, "The University of Toledo: College of Engineering," 7/1/2015. [online]. Available: http://www.eng.utoledo.edu/~rking/IdealTrans.pdf. [Accessed 10/1/2015]

24. "Cadence P-SPICE A/D and Advanced Analysis," Cadence, 10/1/2015. [online]. Available: http://www.cadence.com/products/pcb/spice/pages/default.aspx. [Accessed10/1/2015].

25. D.C. Hamill, "Gyrator Capacitor Modeling: A Better Way of Understanding Magnetic Components," Applied Power Electronics Conference and Exposition, 1994. APEC' 94,Vol.1, pp.326-332, 1994.

26. D.Cheng, L.P.Wong and Y.S. Lee, "Design, Modeling and Analysis of Integrated Magnetics for Power Converters," in IEEE Power Electronics Specialists Conference, APEC'00, pp.320-325, New Orleans,2000.

APPENDIX



Magnetization curve for AKH1 steel[1]

[1] Young, Marcus Aaron II, "Saturable Reactor for Power Flow Control in Electric Transmission Systems: Modeling and System Impact Study. " PhD diss., University of Tennessee, 2015.page95-page104.

Specification for single phase core transformer 500kV/117kV (60Hz)

Primary line voltage =500kV

Phase voltage=500kV/ $(3)^{1/2}$ = 289kV

Primary amplitude voltage =289kV*$(2)^{1/2}$

=408kV (used in simulation)

Secondary line voltage =117kV

Phase voltage=117kV/ $(3)^{1/2}$ =67.5kV

Secondary amplitude voltage =67.5kV*$(2)^{1/2}$

=95kV (resulted voltage in simulation)

Number of turns in Gyrator AC Primary winding= 240

Number of turns in Gyrator AC Secondary winding =56

DC turns in the bias circuit =10

Number of turns in Gyrator DC winding=2000

Branch Parameter:

A_e =2.5µm^2

l_e= 10mm

FOURIER COMPONENTS OF TRANSIENT RESPONSE I(V_Vin)

DC COMPONENT = -5.8681E-03

Harmonic No	Frequency (Hz)	Fourier component	Normalized Component	Phase (Deg)	Normalized Phase (Deg)
1	6.0000E+01	1.6913E+01	1.0000E+00	-8.0048E+01	0.0000E+00
2	1.2000E+02	1.3745E+01	8.1265E-01	1.1171E+02	2.7181E+02
3	1.8000E+02	1.2885E+01	7.6185E-01	-5.7491E+01	1.8265E+02
4	2.4000E+02	1.1253E+01	6.6534E-01	1.3545E+02	4.5564E+02
5	3.0000E+02	9.9676E+00	5.8934E-01	-3.2450E+01	3.6779E+02
6	3.6000E+02	8.3459E+00	4.9346E-01	1.6368E+02	6.4396E+02
7	4.2000E+02	7.0928E+00	4.1937E-01	-1.3677E+00	5.5897E+02
8	4.8000E+02	5.9646E+00	3.5266E-01	-1.6454E+02	4.7584E+02
9	5.4000E+02	5.0012E+00	2.9570E-01	3.3180E+01	7.5361E+02
10	6.0000E+02	4.2468E+00	2.5110E-01	-1.2701E+02	6.7347E+02

TOTAL HARMONIC DISTORTION = 1.6508E+02 PERCENT

VITA

Parul Kaushal was born in India. She earned a Bachelor of Science degree in 2006 from IEET (India) and a Master's of Science degree in electrical engineering from PEC (India) in 2008. She worked for three and half years in a hydro electric designing consulting company before joining University of Tennessee, Knoxville , in 2014 and will be graduating in 2017 with Master's of Science degree in electrical engineering.